Atomic Spectroscopy

January/February 2001 Volume 22, No. 1

In This Issue:

ASPND7 22(1) 235–270 (2001)
ISSN 0195-5373

Issues also available electronically.

(see inside front cover)

Atomic Spectroscopy
Vol. 22(1), January/February 2001

Printed in the United States and published six times a year by:

PerkinElmer Instruments LLC
761 Main Avenue
Norwalk, CT 06859-0226 USA
Tel: +1 (203) 761-2532 • Fax: +1 (203) 761-2898
www.perkinelmer.com

SUBSCRIPTION INFORMATION

Atomic Spectroscopy
P.O. Box 3674
Barrington, IL 60011 USA
Fax: +1 (847) 304-6865

2000 Subscription Rates

- U.S. $60.00 includes third-class mail delivery worldwide; $20.00 extra for electronic file.
- U.S. $80.00 includes airmail delivery; $20 extra for electronic file.
- U.S. $60.00 for electronic file only.
- Payment by check (drawn on U.S. bank in U.S. funds) made out to: "*Atomic Spectroscopy*"

On-line Access

- For electronic file, send request via e-mail to: atsponline@yahoo.com

Back Issues/Claims

- Single back issues are available at $15.00 each.
- Subscriber claims for missing back issues will be honored at no charge within 90 days of issue mailing date.

Address Changes to:
Atomic Spectroscopy
P.O. Box 3674
Barrington, IL 60011 USA

Microfilm

Atomic Spectroscopy issues are available from:
University Microfilms International
300 N. Zeeb Road
Ann Arbor, MI 48106 USA
Tel: (800) 521-0600 (within the U.S.)
+1 (313) 761-4700 (internationally)

Guidelines for Authors

Atomic Spectroscopy serves as a medium for the dissemination of general information together with new applications and analytical data in atomic absorption spectrometry.

The pages of *Atomic Spectroscopy* are open to all workers in the field of atomic spectroscopy. There is no charge for publication of a manuscript.

The journal has around 3000 subscribers on a worldwide basis, and its success can be attributed to the excellent contributions of its authors as well as the technical guidance of its reviewers and the Technical Editors.

A manuscript can be submitted to the editor by mail or e-mail in the following manner:

1. Triplicate, double-spaced.
2. Include abstract for articles.
3. Number the references in the order they are cited in the text.
4. Include bibliography.
5. Submit original drawings or glossy photographs and figure captions.
6. Consult a current copy of *Atomic Spectroscopy* for format.
7. E-mail text in .doc file and graphics in .tif files to the editor: anneliese.lust@perkinelmer.com

All manuscripts are sent to two reviewers. If there is disagreement, a third reviewer is consulted.

Minor changes in style are made in-house and submitted to the author for approval.

A copyright transfer form is sent to the author for signature.

If a revision of the manuscript is required before publication can be considered, the paper is returned to the author(s) with the reviewers' comments.

In the interest of speed of publication, a typeset copy is faxed to the corresponding author for final approval.

After publication, the senior author will receive 50 complimentary reprints of the article.

Additional reprints can be purchased, but the request must be made at the time the manuscript is approved for publication.

Anneliese Lust
Editor, *Atomic Spectroscopy*
PerkinElmer Instruments LLC
761 Main Avenue
Norwalk, CT 06859-0226 USA

Determination of Trace Elements in Coal and Coal Ash Samples by ICP-MS

*Maria Luiza D. P. Godoy[a,b], José Marcus Godoy[a,b], and Luis Alfredo Roldão[a]

[a]Instituto de Radioproteção e Dosimetria, Comissão Nacional de Energia Nuclear
Caixa Postal 37750, Barra da Tijuca, Rio de Janeiro, RJ, Brazil, CEP 22780-970

[b]Departamento de Química, Pontifícia Universidade Católica do Rio de Janeiro,
Rua Marquês de São Vicente 225, Gávea, Rio de Janeiro, RJ, Brazil, CEP 22453-900

ABSTRACT

The determination of several trace elements, including thorium and the lanthanides in coal and coal ashes applying total dissolution and ICP-MS, was studied. The procedures were tested with reference materials (Bituminous Coal NIST 1632a and Fly Ash NIST 1633a). For coal samples, chemical ashing with HNO_3, HF, and $HClO_4$ produces reasonable results. Regarding coal ash samples, some difficulties related to the determination of rubidium, cesium, thorium, and the lanthanides were found and a proposed solution is discussed. Finally, coal, bottom, electrostatic precipitator (ESP), and fly ash samples from a Brazilian coal-fired power plant were analyzed and an enrichment of Mn, Zn, Ge, As, Se, Mo, Cd, Sb, Ag, Pb, Bi, and U in fly ash was observed. The values obtained for refractory elements, such as thorium, cerium, and scandium, in the ESP samples were compared with those obtained by INAA, with good agreement between both results. The use of a large number of elements (57) during the instrument calibration allows the use of the TotalQuant mode as a routine method, instead of the traditional quantitative method, aiming at a trace element environmental monitoring program.

INTRODUCTION

There is great concern about health problems related to trace elements bound to fine particulate materials (1, 2). For this reason, more sensitive analytical techniques, such as inductively coupled plasma optical emission spectrometry (ICP-OES), inductively coupled plasma mass spectrometry (ICP-MS), graphite furnace atomic absorption spectrometry (GFAAS), and instrumental neutron activation analysis (INAA), are discussed in recent works (1-7). Due to the well-known limitation of the viability of a high-flux research reactor close to the laboratory, INAA has its use restricted to a relatively small number of laboratories. Techniques such as ICP-OES require sample digestion before analysis. Slurry nebulization has been proposed by Ebdon et al. (8), but without a clear advantage over digestion methods (3).

The digestion method applied will depend on the mineral phases present in the sample and on the elements of interest. Several works have shown that microwave-assisted digestion procedures in a combination with acids (HNO_3, HCl, H_2SO_4 and $HClO_4$) have given good results (1, 3-7, 9-12) when the elements of interest are those associated with less refractory phases of the samples, such as As, Se, Cu, Cr, Co, Cd, Ni and Pb. However, these procedures could lead to results lower than expected for lanthanides, thorium, and scandium in fly ash samples (3, 7, 10). This limitation can be overcome by using lithium metaborate or lithium tetraborate fusion, which results in highly saline solutions that are incompatible with usual ICP-MS or ICP-OES methodologies, since they require large dilutions and result in high blank values (3, 7, 10). Also volatile element loss with fusion procedures is not very clear; Rodushkin et al. (3) reported low recoveries for elements such as As, Bi, Cd, Pb, Se, and Zn, but the same was not observed by Bettinelli and Barone (7).

The aim of this work is to develop a digestion procedure compatible with ICP-MS which allows the simultaneous determination of thorium and rare earth elements, together with elements such as As, Se, Cu, Cr, Co, Cd, Ni, and Pb, in coal and fly ash samples.

EXPERIMENTAL

Instrumentation

A PerkinElmer SCIEX ELAN® 6000 ICP-MS, equipped with the standard spray chamber and cross-flow nebulizer, was used for the analysis. The instrumental parameters are listed in Table I. The ICP-MS was optimized according to the manufacturer's recommendations. The unique modification was the use of a mass tuning solution, prepared with the addition of Li, Sr, W, Th, and U to the PerkinElmer standard N812-2014 (Ba, Cd, Ce, Cu, Ge, Pb, Mg, Rh, Sc, Tb, and Tl). The final concentration for each element was 10 ng mL^{-1}. A CEM Mars-5 microwave oven was used for sample digestion.

Reagents

- Sub-boiled nitric acid
- Deionized water (18 MΩ, MilliQ™ system, Millipore, Bedford, MA, USA)
- HF suprapur (Merck, Darmstadt, Germany)
- 30% H_2O_2 analytical grade (Peridrol®, Merck, Darmstadt, Germany)
- Lithium Metaborate and Lithium Tetraborate analytical grade (Merck, Darmstadt, Germany)

Standards and Reference Materials

All standard solutions were prepared from 10 mg mL^{-1} PerkinElmer

*Corresponding author.

TABLE I
ICP-MS Operating Conditions

Plasma Conditions	
RF Power	1050 W
Plasma gas flow rate	17 L min^{-1}
Auxiliary gas flow rate	1.2 L min^{-1}
Nebulizer gas flow rate	0.9 L min^{-1}
Sample Uptake Rate	1.0 mL min^{-1}
Measurement Parameters	
Scan mode	Peak Hopping
Lens scanning	Enabled
Detector mode	Dual – Pulse and Analog
Dwell time	50 ms
Number of sweeps per reading	20 (Quantitative) and 6 (TotalQuant)
Number of replicates	3 (Quantitative) and 1 (TotalQuant)

multielement solutions 2, 3, and 5. Two standard reference materials, Bituminous Coal NIST 1632a and Fly Ash NIST 1633a were used. The moisture content was determined on a separate aliquot, dried at 105ºC, resulting in 0.5% for the coal and 0.2% for the fly ash samples.

Calibration

For the TotalQuant™ mode, the system was calibrated using a mixture of the PerkinElmer multielement standard solutions 2, 3, and 5, producing 20 ng mL^{-1} for each element in 2% HNO_3. This mixture contained a total of 57 elements. For the quantitative method, 1, 5, 10 , 15, and 20 ng mL^{-1} solutions were prepared from the PerkinElmer multielement standard solutions. Indium and thallium were added as internal standards to all blanks, sample, and standard solutions to produce a final solution containing 20 ng mL^{-1} of each element.

Applying the quantitative method, the isotopes monitored were ^{52}Cr, ^{53}Cr, ^{55}Mn, ^{60}Ni, ^{63}Cu, ^{65}Cu, ^{66}Zn, ^{68}Zn, ^{75}As, ^{77}Se, ^{82}Se, ^{114}Cd, ^{208}Pb, ^{232}Th, and ^{238}U.

Sample Digestion

The digestion of coal samples was performed in closed Teflon® vessels heated on a hot plate. To a 0.300-g aliquot of each coal sample, 10 mL concentrated HNO_3 was added and left standing overnight without heating. It was heated for 24 hours at 100ºC, then an additional 24 hours at 200ºC. After cooling, 1.5 mL 30% H_2O_2 was added and heated for 24 hours at 200ºC. Then, 2 mL concentrated HF and 0.4 mL concentrated $HClO_4$ were added and again heated for 24 hours at 200ºC. This solution was evaporated to dryness, the residue dissolved with 3.5 mL concentrated HNO_3, and diluted to 50 mL with deionized water.

A 0.300-g aliquot of each ash sample was weighed and transferred to a clean Teflon vessel with 5 mL concentrated HNO_3 and 3 mL concentrated HF. Depending on the number of vessels placed in the microwave oven, the power was adjusted from 300 W (3 vessels) to 1200 W (14 vessels); the hold time was kept constant for 30 minutes. The heating procedure was repeated three times before cooling. After cooling, the solutions were transferred to clean Teflon beakers, 0.2 mL concentrated $HClO_4$ was added, and the solutions evaporated to dryness. The residue was dissolved with 3.5 mL concentrated HNO_3 and diluted to 50 mL with deionized water.

RESULTS AND DISCUSSION

Sample Dissolution Studies

The ICP-MS results for the coal reference sample using the quantitative method are listed in Table II; the TotalQuant mode results are listed in Table III. An acceptance criterion of 10% for certified concentrations and 20% for non-certified concentrations was used. Twenty percent is the criterion used for trace element determinations in environmental samples performed in some interlaboratory studies under the auspices of the U.S. Department of Energy (13).

The results of the proposed method are in good agreement with the certified and non-certified trace element values, including high refractory elements such as thorium, scandium, the lanthanides, tungsten, and titanium (minor constituent). Among 24 elements determined in the coal sample, problems were found only in the determination of Zn (-16%) and Pb (15%) using the quantitative method and Cu (13%) and Pb (20%) applying the TotalQuant mode. As can be seen, the potential interference of $^{40}Ar^{12}C^+$ on $^{52}Cr^+$ and $^{40}Ar^{35}Cl^+$ on $^{75}As^+$ were not observed. Using the quantitative method, Se was close to the quantification limit (1 mg kg^{-1}) as well as Se, Cd, and Sb (2, 0.05, 0.2 mg kg^{-1}) applying the TotalQuant mode. It is important to note the good agreement between the quantitative results and the TotalQuant mode, considered semiquantitative (14). It should also be noted that the ash content in the bituminous coal NIST 1632b is only 6.8%. For this reason, attention needs to be paid to rare earth elements when analyzing coal samples with a high ash content (up to 50%), particularly if refractory minerals such as monazite are present (1, 10).

The analytical results of the fly ash reference sample using the

TABLE II
Determination of Selected Trace Elements in NIST 1632a Bituminous Coal Reference Material Using the Quantitative Method
(Analysis in triplicate, values in mg kg^{-1})

Isotope	Certified value (mg kg^{-1})	Found value (mg kg^{-1})	Bias (%)
^{52}Cr	11[a]	10.23 ± 0.23	-7.0
^{53}Cr	11[a]	10.5 ± 1.6	-4.5
^{55}Mn	12.4 ± 1.0	13.69 ± 0.84	10.4
^{60}Ni	6.10 ± 0.27	6.4 ± 1.5	4.9
^{63}Cu	6.28 ± 0.30	6.35 ± 0.40	1.1
^{65}Cu	6.28 ± 0.30	6.61 ± 0.42	5.3
^{66}Zn	11.89 ± 0.78	8.4 ± 6.4	-29.4
^{68}Zn	11.89 ± 0.78	10.0 ± 6.6	-15.9
^{75}As	3.72 ± 0.09	3.745 ± 0.037	0.7
^{111}Cd	0.0573 ± 0.0027	0.0620 ± 0.018	8.2
^{208}Pb	3.67 ± 0.26	4.24 ± 0.13	15.5
^{232}Th	1.342 ± 0.036	1.354 ± 0.015	0.6
^{238}U	0.436 ± 0.012	0.448 ± 0.015	2.8

[a]-Noncertified value
± signs = 95% confidence ranges

TABLE III
Determination of Selected Trace Elements in NIST 1632a Bituminous Coal Reference Material Using the TotalQuant Mode
(Analysis in triplicate, values in mg kg^{-1})

Element	Certified value (mg kg^{-1})	Found value (mg kg^{-1})	Bias (%)
Li	10[a]	11.6 ± 3.2	16.0
Sc	1.9[a]	2.12 ± 0.35	11.6
Ti	454 ± 17	459 ± 34	1.1
V	14[a]	14.7 ± 1.3	5.0
Cr	11[a]	9.6 ± 2.6	-12.7
Mn	12.4 ± 1.0	12.6 ± 1.6	1.6
Co	2.29 ± 0.17	2.399 ±0.027	4.8
Ni	6.10 ± 0.27	5.97 ± 0.60	-2.1
Cu	6.28 ± 0.30	7.1± 1.3	13.1
Zn	11.89 ± 0.78	12.5 ± 4.3	5.1
As	3.72 ± 0.09	3.55 ± 0.37	-4.6
Rb	5.50 ± 0.11	5.14 ± 0.65	-6.5
Sr	102[a]	100.6 ± 4.4	-1.4
Mo	0.9[a]	0.953 ± 0.067	5.9
Cs	0.44[a]	0.447 ± 0.040	1.6
Ba	67.5 ± 2.1	66.9 ± 3.4	-0.9
La	5.1[a]	4.158 ± 0.094	-18.5
Ce	9[a]	8.61 ± 0.32	-4.3
Sm	0.87[a]	0.774 ± 0.017	-11.0
Eu	0.17[a]	0.166 ± 0.025	-2.4
W	0.48[a]	0.459 ± 0.015	-4.4
Pb	3.67 ± 0.26	4.4 ± 1.8	19.9
Th	1.342 ± 0.036	1.354 ± 0.062	0.9

[a]-Noncertified value
± signs = 95% confidence ranges

quantitative method are shown in Table IV. The results using the TotalQuant mode are listed in Table V. Due to the higher Pb content of the fly ash sample, the observed bias for both methods was lower than for the coal sample. Comparing ^{77}Se and ^{82}Se in Table IV, a positive bias on the first due to $^{40}Ar^{37}Cl^{+}$ was observed. This was not the case with the As results, possibly because of a much higher As content. The difference between the quantitative results and the TotalQuant values is small, indicating the possibility of using this easier method, at least when analyzing environmental samples. Figure 1 shows the values obtained for both samples using the TotalQuant mode vs. the quantitative method. The agreement is very high, except for Zn in the fly ash sample. Values much lower than expected were observed for rubidium, cesium, thorium, and the rare earth elements, indicating incomplete dissolution. A similar problem was reported by Bettinelli and Barone (7). Taking into account not only the potential presence of mineral phases such as monazite, but also the formation of refractory oxides during coal burning, these kinds of problems should be expected (7, 10). It is interesting to note the systematic decrease in the bias from La to Gd and an increase from Gd to Tm. This could in part be explained due to the oxide interference (^{151}Eu and ^{135}BaO, ^{157}Gd and ^{141}PrO) (3).

The procedure was repeated with a centrifugation step after the final dissolution of the residue. The liquid was separated, the solids remaining were weighed, mixed with a 2:1 lithium tetraborate: metaborate mixture equal to twice its mass, and fused in a platinum crucible. After fusion, the residue was dissolved with 1.0 mL concentrated HNO_3 and added to the first solution. The final solution was brought to 50-mL volume with H_2O. Since the fusion was performed

TABLE IV
Determination of Selected Trace Elements in NIST 1633a Fly Ash Reference Material Using the Quantitative Method
(Analysis in triplicate, values in mg kg^{-1})

Isotope	Certified value (mg kg^{-1})	Found value (mg kg^{-1})	Bias (%)
^{52}Cr	198.2 ± 4.7	191 ± 13	-3.6
^{53}Cr	198.2 ± 4.7	195 ± 16	-1.6
^{55}Mn	131.8 ± 1.7	128.1 ± 8.8	-2.8
^{60}Ni	120.6 ± 1.8	117.9 ± 8.4	-2.2
^{63}Cu	112.8 ± 2.6	114.8 ± 7.4	1.8
^{65}Cu	112.8 ± 2.6	120 ± 11	6.4
^{66}Zn	210[a]	211 ± 15	0.5
^{68}Zn	210[a]	229 ± 19	9.0
^{75}As	136.2 ± 2.6	127.6 ± 7.5	-6.3
^{77}Se	10.26 ± 0.17	12.2 ± 2.5	18.9
^{82}Se	10.26 ± 0.17	8.39 ± 0.32	-18.2
^{111}Cd	0.784 ± 0.006	0.768 ± 0.042	-2.0
^{208}Pb	68.2 ± 1.1	59.1 ± 3.3	-13.3
^{232}Th	25.7 ± 1.3	14.8 ± 3.0	-42.4
^{238}U	8.79 ± 0.36	7.80 ± 0.67	-11.3

[a]-Noncertified value
± signs = 95% confidence ranges

TABLE V
Determination of Selected Trace Elements in NIST 1633a Fly Ash Reference Material Using the TotalQuant Mode
(Analysis in triplicate, values in mg kg^{-1})

Element	Certified value (mg kg^{-1})	Found value (mg kg^{-1})	Bias (%)
Sc	41[a]	34.5 ± 2.1	-15.9
Ti	7910 ± 140	7283 ± 904	-7.9
V	295.7 ± 3.6	303 ± 30	2.5
Cr	198.2 ± 4.7	196 ± 21	-1.1
Mn	131.8 ± 1.7	130 ± 12	-1.4
Co	50[a]	53.2 ± 2.1	6.4
Ni	120.6 ± 1.8	140.6 ± 9.4	16.6
Cu	112.8 ± 2.6	116.5 ± 6.5	3.3
Zn	210[a]	171 ± 25	-18.6
As	136.2 ± 2.6	131.8 ± 4.8	-3.2
Rb	140[a]	47.8 ± 6.4	-65.9
Sr	1041 ± 14	989 ± 97	-5.0
Cs	11[a]	5.9 ± 1.8	-46.4
Ba	709 ± 27	636 ± 56	-10.3
La	94[a]	17.5 ± 7.4	-81.4
Ce	190[a]	52 ± 20	-72.6
Nd	85[a]	29 ± 10	-65.9
Sm	20[a]	7.6 ± 1.1	62.0
Eu	4.1[a]	1.91 ± 0.50	-53.4
Gd	13[a]	8.2 ± 1.8	-36.9
Tb	2.6[a]	1.42 ± 0.22	-45.4
Dy	17[a]	8.5 ± 1.2	-50.0
Ho	3.5[a]	1.723 ± 0.099	-50.8
Tm	2.1[a]	0.658 ± 0.040	-68.7
Yb	7.6[a]	4.75 ± 0.20	-37.5
Lu	1.2[a]	0.664 ± 0.052	-44.7
W	5.6[a]	4.81 ± 0.35	-14.1
Pb	68.2 ± 1.1	65 ± 15	-4.7
Th	25.7 ± 1.3	12.5 ± 1.4	-51.4

[a]-Noncertified value
± signs = 95% confidence ranges

only with this final residue, no loss of the volatile elements such as As, Pb, and Se was observed. The values for rubidium, cesium, thorium, and the rare earth elements were much higher than before, but again systematically lower than expected (Table VI), with a bias of about 25% or lower. The systematic decrease on the bias observed from La to Gd and an increase from Gd to Tm was again observed. The introduction of this fusion step not only improved the accuracy but also the precision in the determination of rubidium, cesium, thorium, and the rare earth elements. Of the 15 elements considered environmentally sensitive by Finkelman and Gross (2) and analyzed here using the fusion step, only poor results were obtained for selenium.

The precision was evaluated by pooling the standard deviation obtained for the standard reference material (SRM) together with those obtained for the additional samples below. Elements such as As, Cu, Ni, and Co have a relative standard deviation (RSD) below 5%, while elements such as Zn and rare earth elements have a RSD between 5-10%. The elements Se, Cd, and Sb with concentrations close to the

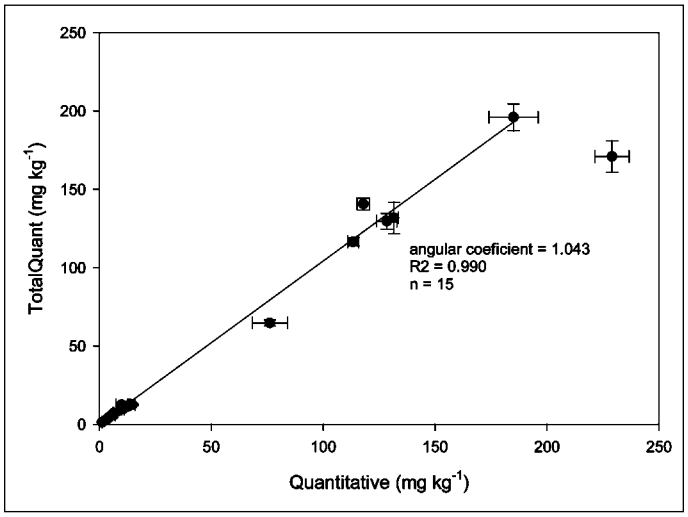

Fig. 1. Comparison between the results obtained using the TotalQuant mode and the quantitative method.

limit of quantification in coal samples show a RSD between 15-20%.

Application of Procedure for Samples From the Thermoelectric Complex Jorge Lacerda (TCJL)

The procedure was applied to three different sets of coal, bottom, and electrostatic precipitator (ESP) ashes from the Thermoelectric Complex Jorge Lacerda (TCJL), Brazil. The values obtained, together with the mean and standard deviations are shown in Table VII. Despite a high ash content in the coal samples (41%), no final residue was observed after the acid digestion procedure. For each element, the bottom ash content was compared with the ESP ash content to verify an enrichment during the burning process and to identify the potentially harmful elements due to an atmospheric release, together with the particulate material. This group of elements includes Zn, Ga, Ge, As, Se, Mo, Cd, Sb, Pb, and Bi. The standard deviation (Table VII) is generally lower than 10%, showing that the blending of coal from the same region (Criciúma, Brazil) leads to a fairly constant trace element concentration. This allows a comparison of the present results to those reported in the TCJL environmental impact assessment report (EIAR, 15) (Table VIII). For the non-volatile elements such as Ti and Ba there is fairly good agreement between both. However, for the volatile elements, the EIAR values have been clearly underestimated, some being even lower in the ESP ash than in the coal, as for Mo, Cd, and Pb.

A composite fly ash, taken from the stack of different TCJL units at different times, was obtained together with GERASUL, the operator of the complex. To evaluate an enrichment in the fly ash, the mean concentration in coal (Table VII) was normalized to barium (Coal Normalized Concentration, CNC) as well as the concentration in the fly ash (Fly Ash Normalized Concentration, FANC). An enrichment factor was calculated by dividing the normalized fly ash concentration by the normalized coal concentration. Since the coal concentration is a mean value and the fly ash sample is a composite sample, as described above, it was decided to define "enriched" in the fly ash those elements with an enrichment factor larger than 1.5. To this group belong Mn, Zn, Ge, As, Se, Mo, Ag, Cd, Sb, Bi, and U.

A similar approach was tested using the coal concentration normalized to the ash content (41%), here called Potential Residue Concentration (PRC). Using an enrichment factor calculated and based on this PRC, Pb is added to the previous group and, somewhat surprisingly, the rare earth elements as well as Sc and Y (Table IX) are also added. Since similar inconsistency occurs using data from other power plants (17), it was decided to change from 1.5 to 2 for this second evaluation. After that, the results observed are the same for both approaches. The absence of Pb among these elements can also indicate a release of this element in gaseous form, which could also explain the low enrichment factor observed for several volatile elements such as As and Cd.

Additionally, 250-mg aliquots from two ESP ash samples were irradiated for two hours on a swimming pool research reactor under a thermal flux of $1x10^{12}$ neutrons$\cdot cm^{-2}\cdot s^{-1}$, together with 250-mg aliquots of NIST 1633a reference material as a comparative standard. About 20 days later, gamma spectrometry measurement was performed using a 40% relative efficiency intrinsic germanium detector, 5 cm sample detector distance and two hours counting time. The concentration of each element was calculated using the relative method (16); the results are presented in Table X. Figure 2 shows the ICP-MS results against the INAA values, which shows that there is good correlation between both methods ($R^2 = 0.997$); the ICP-MS results, on average, about 10% lower than the INAA results.

TABLE VI
Determination of Rubidium, Cesium, Thorium and Rare Earth Elements in Fly Ash Reference Material NIST 1633a, With the Additional Fusion of the Residue with (LMB+LTB), Using TotalQuant Mode
(Analysis in triplicate, values in mg kg^{-1})

Element	Certified value (mg kg^{-1})	Found value (mg kg^{-1})	Bias (%)
Rb	140[a]	110 ± 17	-21.4
Cs	11[a]	8.6 ± 1.3	-21.8
La	94[a]	71 ± 20	-24.5
Ce	190[a]	153 ± 45	-19.3
Nd	85[a]	74 ± 11	-19.5
Sm	20[a]	14.6 ± 1.2	-27.0
Eu	4.1[a]	3.30 ± 0.20	-19.5
Gd	13[a]	15.73 ± 0.70	21.0
Tb	2.6[a]	2.277 ± 0.050	-12.4
Dy	17[a]	12.34 ± 0.45	-27.4
Ho	3.5[a]	2.47 ± 0.15	-29.4
Tm	2.1[a]	0.953 ± 0.025	-54.6
Yb	7.6[a]	5.98 ± 0.17	-21.3
Lu	1.2[a]	0.872 ± 0.035	-27.3
Th	25.7 ± 1.3	22.6 ± 2.0	-12.1

[a]-Noncertified value
± signs = 95% confidence ranges

TABLE VII

Trace Elements in Coal, Bottom, and Electrostatic Precipitator (ESP) Ash Samples from TCJL Brazil

(Individual values, mean and standard deviation in mg kg^{-1})

Element	Coal			Bottom ash			ESP ash		
Li	52.95	51.81	51.87	103.5	134.0	113.9	102.3	113.1	116.1
	52.21(0.37)			117.1(8.9)			10.5(4.2)		
Sc	7.4	4.5	11.1	39.0	51.0	31.7	31.2	34.2	34.6
	7.6(1.9)			40.6(5.6)		33.4(1.1)			
Ti	2097	2213	4257	$8.7x10^3$	$1.2x10^4$	$7.4x10^3$	$7.5x10^3$	$8.1x10^3$	$8.0x10^3$
	2856(702)			9.2x103(1.3x10^3)			7.9x103(1.8x10^2)		
V	89.3	98.1	118	215	262	261	227	251	277
	101.9(8.6)			246(16)			252(15)		
Cr	64.6	66.3	72.4	141	177	158	144.8	167.1	168.2
	67.8(2.4)			159(10)			160.0(7.6)		
Mn	108.7	91.75	111	259	326	244	219	250	207
	103.8(6.1)			276(25)			225(13)		
Co	7.26	8.13	8.43	18.3	23.9	20.1	15.52	17.25	15.89
	7.94(0.35)			20.8(1.6)			16.22(0.52)		
Ni	19.08	21.30	21.98	48.6	61.5	50.2	42.2	46.0	42.4
	20.79(0.87)			53.4(4.1)			43.5(1.2)		
Cu	24.70	22.48	23.81	55.8	62.5	44.7	51.2	51.4	48.2
	23.66(0.64)			54.4(5.2)			50.3(1.0)		
Zn	120	81.5	117	168	153	91.6	261	322	225
	106(12)			138(23)			270(28)		
Ga	15.2	15.4	19.2	25.75	26.50	24.23	36.6	45.6	47.1
	16.6(1.3)			25.50(0.67)			43.1(3.3)		
Ge	6.78	7.30	8.42	14.6	13.0	7.42	14.9	19.5	22.9
	7.50(0.49)			11.7(2.2)			19.1(2.3)		
As	15.2	13.0	16.9	4.61	4.62	2.63	26.9	40.0	36.4
	15.0(1.1)			3.95(0.66)			34.4(3.9)		
Se	4.02	2.93	3.24	3.89	4.65	2.26	6.9	8.1	3.4
	3.40(0.32)			3.60(0.70)			6.1(1.4)		
Rb	40.0	37.6	31.6	156	179	117	131.9	120.2	131.3
	36.4(2.5)			151(18)			127.8(3.8)		
Sr	34.4	27.7	39.7	91.6	91.7	96.7	92.8	95.4	83.4
	33.9(3.5)			93.3(1.7)			90.5(3.7)		
Y	16.9	13.4	13.8	89.9	116	83.2	77.1	81.3	82.6
	14.7(1.1)			96.2(9.9)			80.4(1.7)		
Mo	2.42	2.05	2.73	2.19	2.61	2.30	4.85	5.87	6.71
	2.40(0.20)			2.37(0.13)			5.81(0.54)		
Ag	0.40	0.40	0.42	0.78	0.99	0.71	0.84	0.92	0.92
	0.41(0.01)			0.83(0.09)			0.90(0.03)		
Cd	0.44	0.32	0.40	0.27	0.12	0.09	0.91	1.06	0.85
	0.39(0.04)			0.16(0.05)			0.94(0.06)		

Table VII continued on next page

Table VII continued

Element	Coal			Bottom ash			ESP ash		
Sb	0.66 0.87(0.22)	0.64	1.30	0.91 0.79(0.10)	0.58	0.87	1.36 2.07(0.55)	1.69	3.14
Cs	8.24 8.30(0.41)	7.62	9.04	27.6 27.2(3.4)	32.8	21.1	23.3 22.7(1.2)	20.4	24.5
Ba	236 225(11)	238	203	494 574(84)	742	487	507 539(49)	636	474
La	19.7 15.8(2.1)	15.1	12.7	111 118(14)	145	99.0	91.3 94.9(2.5)	93.9	99.6
Ce	39.6 35.1(2.3)	33.8	32.0	236 254(31)	315	210	193.9 202.9(4.6)	206.8	208.1
Pr	5.25 4.45(0.40)	4.13	3.96	27.0 28.9(3.6)	35.8	23.8	21.5 21.9(0.2)	21.9	22.1
Nd	19.7 16.9(1.4)	15.8	15.2	104 110(14)	136	89.4	82.9 85.6(1.4)	86.7	87.3
Sm	4.17 3.64(0.27)	3.44	3.30	20.8 22.5(3.0)	28.4	18.3	15.43 15.66(0.16)	15.97	15.58
Eu	0.87 0.76(0.05)	0.71	0.70	4.05 4.41(0.60)	5.58	3.60	3.07 3.12(0.04)	3.20	3.10
Gd	4.71 4.00(0.36)	3.67	3.61	22.2 24.0(3.6)	31.0	18.9	17.06 18.00(0.91)	19.83	17.12
Tb	0.68 0.60(0.04)	0.55	0.56	2.85 3.17(0.41)	3.98	2.67	2.44 2.58(0.17)	2.92	2.39
Dy	3.89 3.36(0.27)	3.17	3.03	18.5 19.2(2.9)	24.5	14.6	13.66 14.57(0.87)	16.31	13.73
Ho	0.82 0.71(0.06)	0.65	0.65	3.55 3.73(0.49)	4.65	2.97	2.70 2.96(0.22)	3.39	2.79
Er	2.10 1.86(0.14)	1.63	1.86	9.83 11.0(1.3)	13.6	9.43	9.25 8.45(0.40)	8.04	8.07
Tm	0.35 0.31(0.02)	0.30	0.29	1.53 1.60(0.21)	1.99	1.28	1.17 1.34(0.09)	1.44	1.42
Yb	2.20 1.99(0.11)	1.85	1.91	10.2 10.5(1.5)	13.3	8.17	8.90 9.28(0.20)	9.56	9.39
Lu	0.35 0.31(0.02)	0.30	0.30	1.44 1.54(0.17)	1.88	1.3	1.09 1.19(0.08)	1.35	1.12
W	2.03 1.92(0.06)	1.85	1.87	3.75 3.67(0.42)	4.34	2.91	4.72 4.65(0.27)	5.07	4.15
Pb	31.26 30.18(0.70)	28.86	30.43	39.9 31.3(4.5)	29.1	24.9	66.6 73.0(4.3)	71.5	81.0
Bi	0.70 0.72(0.02)	0.76	0.71	0.64 0.38(0.13)	0.32	0.20	1.54 1.74(0.18)	2.01	1.6
Th	9.88 8.91(0.73)	9.37	7.49	50.7 52.9(6.0)	64.3	43.8	35.39 35.50(0.10)	35.44	35.68
U	6.02 5.97(0.18)	5.64	6.26 22.6(2.2)	21.8	26.7	19.4	17.35 17.36(0.54)	16.43	18.31

TABLE VIII
Comparison Between Trace Elements Content Found in This Work and Those Reported on the TCJL Environmental Impact Assessment report (EIAR) (values in mg kg^{-1})

Element	Coal		ESP ash	
	This work	EIAR	This work	EIAR
Ti	2856	3900	7900	7800
V	102	120	252	310
Cr	68	74	160	150
Mn	104	124	225	210
Co	7.9	10	16	19
Ni	21	30	44	61
Cu	24	32	50	56
Zn	106	217	270	233
As	15	2.8	34	13
Se	3.4	3.9	6.1	3.6
Mo	2.4	11	5.8	7.0
Cd	0.39	0.9	0.94	0.4
Sb	0.87	0.8	2.1	1.4
Ba	225	215	539	445
Pb	30	48	73	26
Th	8.9	25	36	<30
U	6.0	2.5	17	3.4

TABLE IX
Enrichment Factors Based on Barium Normalized Concentrations (CNC and FANC) and on Potential Residue Concentration (PRC)
(Concentrations in mg kg^{-1})

Element	Coal	CNC	Fly ash	FANC	FANC/CNC	PRC	Fly ash/PRC
Sc	7.6	0.0338	34.6	0.0463	1.37	18.5	1.87
Ti	2856	12.69	6744	9.03	0.71	6967	0.97
V	102	0.453	297	0.398	0.88	249	1.19
Cr	67.8	0.301	187	0.250	0.83	165	1.13
Mn	103.8	0.461	686	0.918	**1.99**	253	**2.71**
Co	7.94	0.0353	16.9	0.0226	0.64	19.4	0.87
Ni	20.8	0.0924	55.2	0.0739	0.80	50.7	1.09
Cu	23.7	0.1053	56.7	0.0759	0.72	57.8	0.98
Zn	106	0.471	538	0.720	**1.53**	259	**2.08**
Ga	16.6	0.0738	71.4	0.0956	1.30	40.5	1.76
Ge	7.5	0.0333	56.8	0.0760	**2.28**	18.3	**3.10**
As	15	0.0667	94.3	0.1262	**1.89**	36.6	**2.58**
Se	3.4	0.0151	58.1	0.0778	**5.15**	8.3	**7.00**
Rb	36.4	0.162	102	0.137	0.85	88.8	1.15
Sr	33.9	0.151	121	0.162	1.07	82.7	1.46
Y	14.7	0.0653	66.1	0.0885	1.36	35.9	1.84
Mo	2.4	0.0107	17.4	0.0233	**2.18**	5.9	**2.95**
Ag	0.41	0.0018	2.88	0.0039	**2.17**	1.0	**2.88**
Cd	0.39	0.0017	2.62	0.0035	**2.06**	0.95	**2.76**
Sb	0.87	0.0039	4.94	0.0066	**1.69**	2.1	**2.92**
Cs	8.3	0.0369	20.6	0.0276	0.75	20.2	1.02
Ba	*225*	*1.000*	*747*	*1.000*	*1.00*	*549*	*1.36*
La	15.8	0.0702	64.7	0.0866	1.23	38.5	1.68
Ce	35.1	0.156	137	0.183	1.17	85.6	1.60
Pr	4.45	0.0198	16.1	0.0216	1.09	10.9	1.48
Nd	16.9	0.0751	59.3	0.0794	1.06	41.2	1.44
Pb	30.2	0.134	142	0.190	1.42	73.7	1.93
Bi	0.72	0.0032	3.58	0.0048	**1.50**	1.8	**1.99**
Th	8.91	0.0396	29.8	0.0399	1.01	21.7	1.37
U	5.97	0.0265	30.1	0.0403	**1.52**	14.6	**2.06**

CONCLUSION

Instrument calibration with a large number of elements (57) allows the use of the TotalQuant mode as a routine method, instead of the traditional quantitative method, for the development of a trace element environmental monitoring program.

Reasonable results for elements such as As, Se, Cd, and Pb in coal and fly ash samples are achievable using an acid digestion method. The same results were found in the determination of refractory elements in coal. Due to the elevated sensitivity of ICP-MS for the determintation of thorium and the rare earth elements, and the fact that large sample dilutions can be made, a separate aliquot, dissolved by LMB or LTB fusion, seems to be the correct choice for the determination of these elements of fly ash samples. This also avoids volatile elements loss and instrument damage due to the use of highly saline solutions.

ACKNOWLEDGMENTS

The present work was partially supported by the Conselho Nacional de Desenvolvimento Científico e Tecnológico (CNPq) under the research contract number 460958/2000-3. The authors would like to express our thanks to José Magri and Ligia, from GERASUL, for the local support and the samples from the Thermoelectric Complex Jorge Lacerda (TCJL)

Received January 5, 2001.

TABLE X
Comparison Between Trace Element Content in TCJL Fly Ash Samples Obtained by ICP-MS and INAA (Values in mg kg^{-1})

Element	INAA	ICP-MS	Difference (%)
Sc	37.4 40.1	31.21 34.2	-16.6 -14.7
Cr	151 170	144.8 167.1	-4.1 -1.7
Co	18.0 20.7	15.52 17.25	-13.8 -16.7
Zn	290 351	261 322	-10.0 -8.5
Se	6.2 5.1	6.9 8.07	11.3 58.2
Rb	149 133	131.9 120.2	-11.5 -9.6
Sb	1.8 2.6	1.360 1.691	-24.4 -35.0
Cs	28.0 26.0	23.31 20.36	-16.8 -21.7
Ce	231 231	193.9 206.8	-16.1 -10.5
Eu	3.65 3.77	3.070 3.200	-15.9 -15.1
Tb	3.07 2.73	2.440 2.920	-20.5 7.0
Th	39.1 38.5	35.39 35.44	-9.5 -7.9

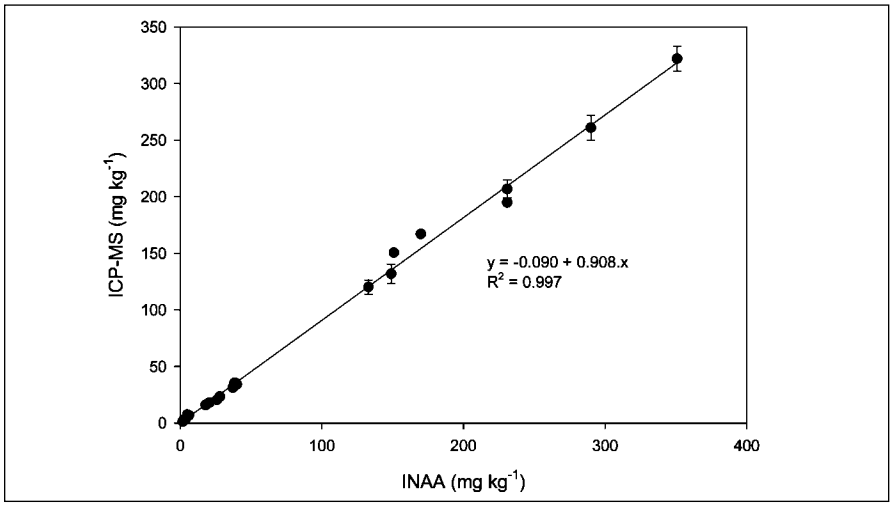

Fig. 2. Comparison between the electrostatic precipitator (ESP) ash results obtained by ICP-MS and by Instrumental Neutron Activation Analysis (INAA).

REFERENCES

1. A.I. Karayigit, R.A. Gayer, X. Querol and T. Onacak, International Journal of Coal Geology 44, 169 (2000).
2. R.B. Finkelman and P.M.K. Gross, International Journal of Coal Geology 40, 91 (1999).
3. I. Rodushkin, M.D. Axelsson, E. Burman, Talanta 51, 743 (2000).
4. E. Hatanpää, K. Kajander, T. Laitinen, S. Piepponen and H. Revitzer, Fuel Processing Technology 51, 205 (1997).
5. E. Häsänen, L. Aunela-Tapola, V. Kinnunen, K. Larjava, A. Methonen, T. Salmikangas, J. Leskelä and J. Loosaar, The Science of the Total Environment, 198, 1 (1997).
6. R.A. Gayer, M. Rose, J. Dehner and L.Y. Shao, International Journal of Coal Geology, 40, 151 (1999).
7. M. Bettinelli and U. Baroni, Atomic Spectrosc. 16, 203 (1995).
8. L. Ebdon, M.E. Foulkes, H.G.M. Parry, C.T. Tye, Journal of Analytical Atomic Spectrometry 3, 753 (1988).
9. F.E. Smith and E.A. Arsenault, Talanta 43, 1207 (1996).
10. R.I. Botto, Spectrochimica Acta 14, 141 (1991).
11. M. Bettinelli, U. Baroni and N. Pastorelli, Journal of Analytical Atomic Spectrometry 3, 1005 (1988).
12. J. Alvarado, L.E. León, F. López and C. Lima, Journal of Analytical Atomic Spectrometry 3, 135 (1988).
13. U.S. Department of Energy, Mixed Analyte Performance Evaluation Program, MAPEP Handbook, February 2000, p. 25.
14. PERKIN-ELMER SCIEX, ELAN 6000 Software Guide, Part Number 0993-8968 Rev. F, June 1997.
15. GERASUL, Complexo Termelétrico Jorge Lacerda, Unidade IV, Relatório de Impacto Ambiental Vol. 2, Fundação Universidade-Empresa de Tecnologia e Ciências, Universidade Federal do Rio Grande do Sul, Caixa Postal 1311, Porto Alegre, Rio Grande do Sul, Brasil, 1987.
16. J.M. Godoy in A. Mudroch, J.M. Azcue and P. Mudroch (ed.) Manual of Physico-Chemical Analysis of Aquatic Sediments, CRC Lewis, p. 287 (1996).
17. J.H. Horton, R.S. Dorsett and R.E. Copper, Trace Elements in the Terrestrial Environment of a Coal Fired Powerhouse, Report DP-1475/UC-11, September 1977.

Determination of Total Sulphur in Gasoline by ICP-OES

***Kerry C. Weston, Zeochem Molecular Sieves**
1314 South 12th Street, Louisville, KY 40210 USA
and
David R. Hilligoss, PerkinElmer Instruments
761 Main Avenue, Norwalk, CT 06859 USA

ABSTRACT

Sulphur in gasoline was analyzed by simultaneous ICP-OES using a modified, cooled spray chamber. ASTM procedures, regulatory limits and different approaches to standardization are discussed. ICP-OES results on NIST certified samples show good agreement with existing ASTM procedures.

INTRODUCTION

The presence of sulphur has no intrinsic value in automotive fuel. It is there mainly as an impurity of the crude oil used to make gasoline. There are several refinery steps that reduce the level of sulphur but significant concentrations still remain in the final blends. In the United States, the sulphur content of gasoline ranges from 50 to 600 mg/kg, while in Canada, the average concentration (1997) is 360 mg/kg. Automobiles have always emitted sulphur oxides (a key component of acid rain), but these emissions were considered negligible compared to stationary sources of sulphur oxides. As a result, the sulphur content of gasoline was not an issue until post-combustion emission control devices (catalytic converters) were introduced in the 1970s (1).

The first laws governing exhaust emissions by automobiles were set in the United States through the Clean Air Act of 1968. Reacting to the severe smog problems in California, the state was granted the authority to set its own emission standards. The state chose to set much more stringent emission standards than those set by the U.S. Environmental Protection Agency (EPA). In 1976, California introduced limits on sulphur in gasoline (Table I).

TABLE I
California Sulphur Limits

Year	Regulatory Limit
1976	500 mg/kg per gallon
1978	400 mg/kg per gallon
1980	300 mg/kg per gallon
1996	30 mg/kg per gallon***

***The 1996 specification was set with an average limit of 30 mg/kg per gallon and a maximum of 80 mg/kg per gallon. These limits were not set to target the sulphate emissions rather to maximize the efficiency of the automotive three-way catalytic converter (1).

The Canadian government has followed the Californian model in setting sulphur specifications. In October of 1998, the government issued a mandate that the level of sulphur be reduced from 360 mg/kg (1998) to 30 mg/kg per liter average and a maximum value of 80 mg/kg per liter by 2005 (1).

The Environmental Protection Agency Tier 2 proposal specifies 30 mg/kg sulphur in gasoline (80 mg/kg cap.) for large refiners by 2004 (2).

With tougher specifications looming, it has become very important that reliable testing methods for sulphur be established for not only regulatory bodies, but for researchers as well. The EPA requires that ASTM D 2622 (wavelength dispersive X-Ray) be used for low level sulphur determinations. However, the California Air Resources Board (CARB) has approved ASTM D 5453 (UV-fluorescence) for use (2).

Reacting to the need to research this potential growth market, we developed a method utilizing radially viewed inductively coupled plasma optical emission spectrometry (ICP-OES) for total sulphur determinations.

EXPERIMENTAL

Instrumentation

All experiments were conducted using a PerkinElmer™ Optima 3000™ RL inductively coupled plasma optical emission spectrometer with a PerkinElmer AS-91 autosampler. Modifications made to the standard system were as follows:

1. Cross-flow nebulizer was replaced with a K3 Meinhard® nebulizer (J.E. Meinhard Associates Inc., 1900 J East Warner Avenue, Santa Ana, CA, 92705).

2. Scott spray chamber was replaced with a cyclonic spray chamber (Precision Glassblowing, 14775 East Hinsdale Ave., Englewood, CO, 80112, part no. 300-19).

3. Standard spray chamber mount was replaced with the dry aerosol mount (part no. N069-0637) for attaching the cyclonic spray chamber. O-Rings required are part no. 0990-2152.

4. Standard Alumina injector (2.0 mm) was replaced with a 0.85-mm Alumina injector (part no. N058-2186).

5. Standard single-slot quartz tube was replaced with a three-slot quartz tube (part no. N068-1690).

6. Recirculating chiller capable of achieving –10 ºC.

7. Red/red Viton pump tubing (part no. NC9663033) from Cole-Parmer.

**Corresponding author.*

Reagents

1. Kerosene GR certified less than 1 mg/kg S (EM Science 480 S. Democrat Road, Gibbstown, NJ 08027 USA , part no. KX0020-3).

2. Calibration standards of sulphur in iso-octane (Alfa Aesar, 30 Bond Street, Ward Hill, MA 01835-8099 USA).

3. 1000 mg/kg Cr in xylenes (Alfa Aesar).

4. NIST 2724a, NIST 2724b, and NIST 2294-2297 used for calibration and evaluation of method accuracy (National Institute of Standards and Technology, Gaithersburg, MD 20899-0001 USA).

5. Calibration standards of sulphur in gasoline (Analytical Services, Inc., PO Box 7895, The Woodlands, TX 77387 USA, phone (281) 419-9229).

Instrument and Method

This study was performed using the PerkinElmer Optima 3000 RL ICP-OES configured for radial viewing. The instrumental conditions used for this study are given in Table II.

The jacketed spray chamber was cooled to –5ºC using a Fisher-brand recirculating chiller. This was found to be the optimum temperature with respect to sample equilibration and rinse-out time. At the chilled conditions, solvents become more viscous and pump noise can be seen in the plasma. To eliminate this noise, the peristaltic pump was removed from the sample introduction system and the K3 nebulizer was allowed to aspirate at its own rate. The matrix of the samples and standards was matched as closely as possible to eliminate matrix effects, but an internal standard of chromium was also added to monitor any sample transport problems.

High-purity kerosene available from E.M. Science (Optima grade) was used as the solvent for the experiment. All standards and samples were diluted 1:10 on a weight-to-weight basis. The standards from Alfa Aesar were used to calibrate the unit. The standards used for the experiment were 0 mg/kg, 100 mg/kg, 300 mg/kg, and 600 mg/kg sulphur in iso-octane. Diluting by 10 yields actual concentrations of 0 mg/kg, 10 mg/kg, 30 mg/kg, and 60 mg/kg. A spiking standard containing 1000 mg/kg sulphur in kerosene was used to make standard additions into the samples.

TABLE II
Instrument Operating Conditions

Parameter	Radial Setup
Plasma Gas	20.0 L/min
Auxiliary Gas	2.0 L/min
Nebulizer Gas	0.3 – 0.4 L/min
Power	1500 Watts
Nebulizer Type	Meinhard K3
Spray Chamber	Jacketed Cyclonic
Uptake Rate	1.0 – 2.0 L/min

TABLE III
Data Collection Conditions

Element	Read Time	Int. Time	Wavelength	Background Point 1	Background Point 2
S	15 sec	0.5 sec	180.669 nm	-0.014 nm	0.014 nm
Cr	15 sec	0.5 sec	267.716 nm	-0.032 nm	0.033 nm

The wavelengths used are the same as those used for aqueous analyses; however, the background structure resulting from the organic matrix differs slightly from that of an aqueous analysis. Therefore, background points must be selected to best suit the sample type (Table III).

RESULTS AND DISCUSSION

When this procedure was developed, various problems were encountered. First and foremost, the sample introduction system needed to be modified, so that it could accommodate the iso-octane sample matrix. Introduction of this sample component without chilling the system causes the plasma to extinguish. This is due to the very high vapor pressure associated with gasoline (iso-octane). Cooling the sample introduction system permits the gasoline to behave in much the same way as kerosene. This was achieved by removing the standard Scott Type spray chamber and replacing it with a jacketed cyclonic spray chamber. Rinse-out times, sample equilibration times, and memory effects all played a role in switching from a Scott Type chamber to a cyclonic chamber. The experiments using a radially configured cooled Scott Type chamber showed excessive rinse-out time (greater than 10 minutes) and sample equilibration time (greater than 15 minutes).

Organic compounds nebulize much more efficiently than aqueous compounds. This makes it a necessity to restrict the flow to the plasma. In typical aqueous samples, a standard cross-flow nebulizer is used in conjunction with a 2-mm alumina injector. We found that a .85-mm injector is much better at limiting the sample flow. We also needed to move from a nebulizer gas flow of 0.95 L/min (aqueous) down to 0.3 to 0.4 L/min. To achieve this, a low-flow Meinhard® nebulizer was used. It was allowed to self-aspirate in order to eliminate pump noise. Obviously, gasoline-resistant pump tubing needed to be used.

After setting up the sample introduction system, attention was turned to optimizing the plasma conditions. Several conditions must be considered when optimum plasma conditions are being established. First and foremost, a stable, robust plasma is required. To achieve this, the power and the plasma gas flow are set to their maximum operating condition (1500 Watts and 20 L/min).This creates a very "stiff" plasma and is not extinguished with the 10% isooctane. This condition also creates a more stable environment and leads to improved precision. The auxiliary gas flow is set to its maximum condition of 2 L/min, which moves the plasma off the injector, thus reducing carbon buildup.

Now, the plasma must be aligned for optimum sulphur viewing. The system has two variables that can be controlled, the X and Y axis (Figure 1).

The normal analytical zone (NAZ) for ICP is generally 15 to 25 mm above the load coil. In this region, excited ions are analyzed. For most analytes, there is equilibrium between atomic emissions and ionic emissions. This equilibrium is generally 90% ionic (a type II transition) and 10% atomic (a type I transition). The equilibrium is dependent on the sample matrix, the plasma conditions and, obviously, on the analyte.

In our case, we were examining the emission lines for sulphur, which are very low-level atomic lines. The atomic lines are more prominent in the initial radiation zone (IRZ), which occurs much lower in the plasma, generally from 1 to 15 mm above the load coil. By moving our viewing location, we were able to extract more signal from our sample, thus improving our relative precision and detection limits.

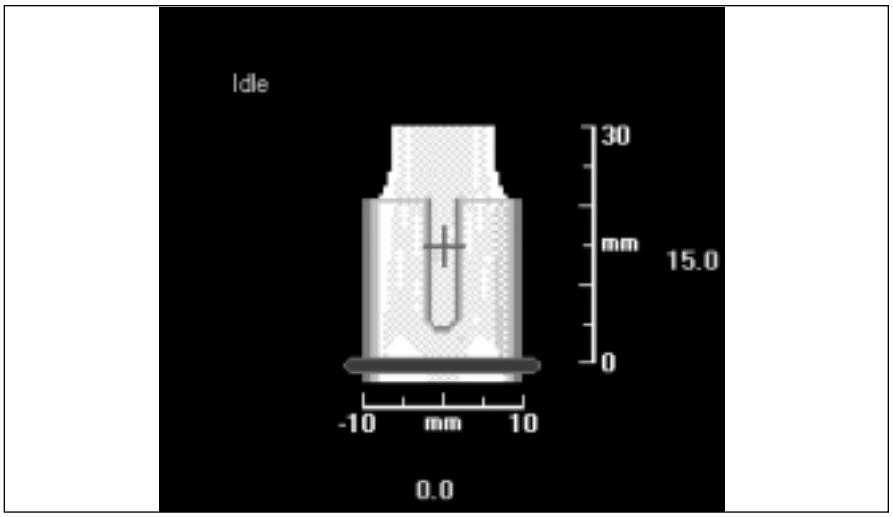

Fig. 1. Normal Torch Viewing

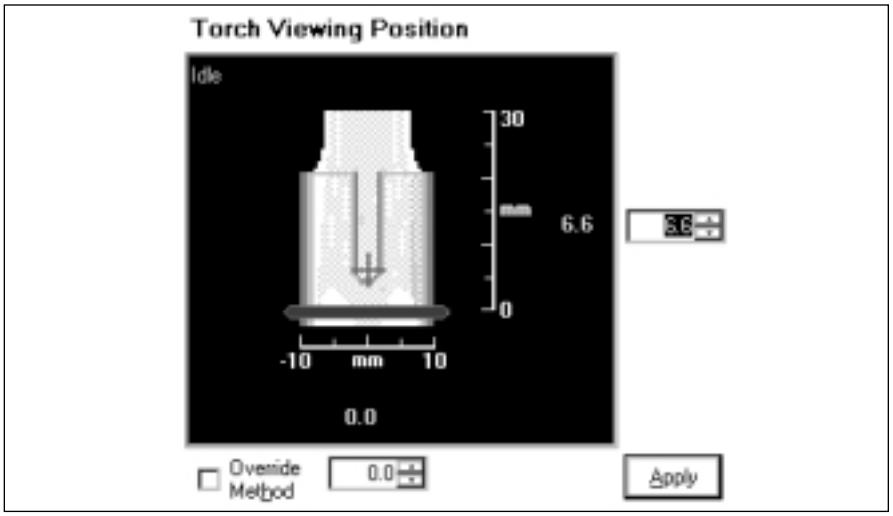

Fig. 2. Adjusted Torch Viewing.

The torch was adjusted to optimum viewing height of 6.6 mm above the load coil (Figure 2). This was based on an experiment using 10 mg/kg sulphur spike with nominally 10 mg/kg chromium. The sample was analyzed over the range of 0 to 30 mm above the load coil. The resulting data plot is shown in Figure 3. At about 6.6 mm, the relative S/Cr ratio is 1, which means at that height, on the relative scale, the plasma efficiency for both sulphur and chromium is nominally the same, thus making it a good choice for analysis.

Once the proper plasma conditions are chosen, it is possible to perform the analysis. The following analytical methods were evaluated:

1. Direct calibration using NIST standards

2. Direct calibration using isooctane standards

3. Method of standard additions

4. Direct calibration using gasoline standards

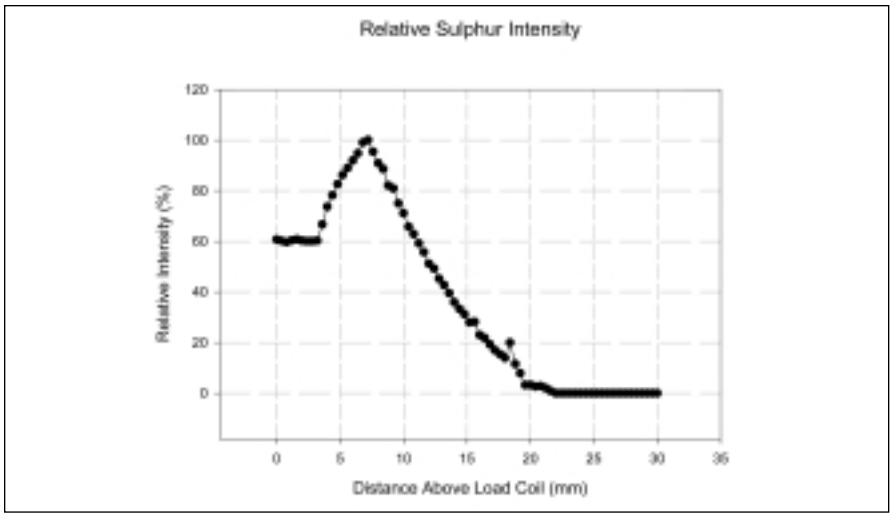

Fig. 3. Intensity as a Function of Viewing Heigbt.

TABLE IV
NIST Standards

SRM #	Matrix	Concentration (mg/kg)
2294	RFG w/ 11% MTBE	35
2295	RFG w/ 15% MTBE	300
2296	RFG w/ 13% ETBE	35
2297	RFG w/ 10% Ethanol	300

TABLE V
Precision Comparison of ICP and ASTM Methods

Range (mg/kg)	D 5453	D 2622	ICP
0-10	6.6	10.8	< 10.0
11-25	4.9	10.6	< 5.0
26-50	4.8	9.8	< 5.0
51-100	4.8	6.8	< 2.0
101-200	4.4	6.4	< 1.0

Calibration Using NIST Standards

The National Institute of Standards and Technology (NIST) offers four different standard reference samples (SRM), which can be used for determining sulphur in gasoline (see Table IV).

For our calibration, we used SRM 2294 and SRM 2295. We found the curve to be linear, but the results obtained from that analysis were about half of other ASTM methods. The analysis of SRM 2297 using that calibration curve was also very low, 178 mg/kg or 59% recovery. This is a very good example of sample-to-standard matrix effects. The SRMs contain a synthetic blend of hydrocarbons, mimicking the concentrations found in gasoline. The blend is then spiked with n-butylsulfide to achieve the desired sulphur content. Very early in the process, we eliminated the NIST standards as a possible standardization source.

Calibraton Using ISO-Octane Standards

Still searching for a calibration source, we elected to purchase materials from Alfa Aesar. They supply high-quality standards for trace metal oil analysis and recently introduced a set of sulphur standards in iso-octane. We elected to use standards at 30 mg/kg, 50 mg/kg, 100 mg/kg, 300 mg/kg, and 600 mg/kg. These standards are traceable to NIST SRM 2724a, sulphur in diesel fuel oil. We found that this standard curve provided a wide dynamic range and the results were very comparable to other ASTM methods. The calibration curve is linear over the range of 0 to 600 mg/kg with a Pearson value of 0.9999. Matrix effects are still a problem when using this material, as the iso-octane matrix does not "match" the gasoline samples perfectly. The results using this method are often skewed high, by as much as 25%. Straight iso-octane does not nebulize as effectively as the gasoline samples. The use of an internal standard does not seem to help compensate for these differences. However, we found that this method was still very good in measuring relative differences between samples. The method was found to have very good precision, comparable to ASTM D-5453, and much better than ASTM D-2622 (see Table V).

Method of Standard Additions

In order to remove the matrix as a part of the analysis, we decided to use the method of standard additions. For this analysis, there is no "traditional" calibration curve, rather a set of sample spikes used to determine the sample concentration. To perform this, we used 3 g of sample, diluted to 30 g with kerosene (9 parts kerosene, 1 part gasoline). This was the initial sample. Then we used a standard containing 1000 mg/kg sulphur in kerosene as a spiking agent. The spike amount varied from 0.05 g to 0.5 g, depending on the approximate sample concentration, but we were always careful to keep the

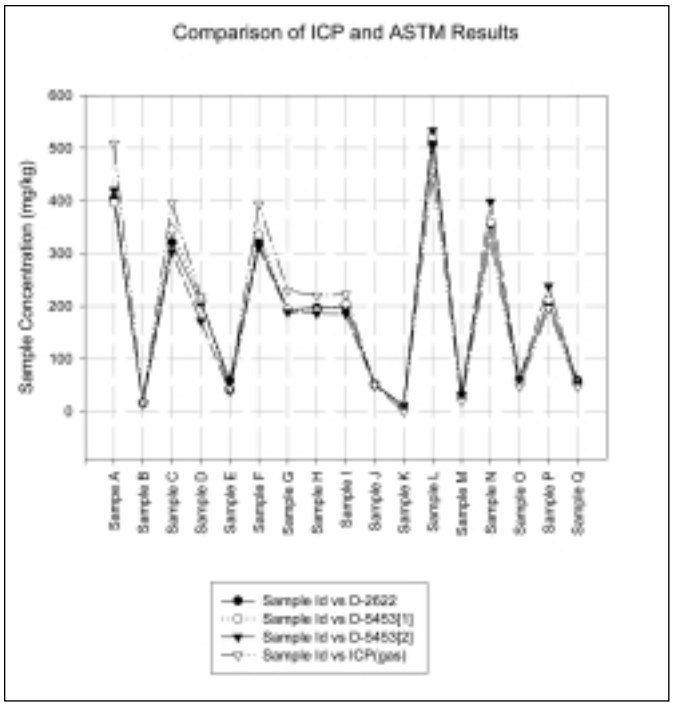

Fig. 4. ICP vs. ASTM using sulphur in gasoline standards.

TABLE VI
Results Compared to ASTM Methods

Sample ID	D 2622	D 5453	ICP (Cal.)	ICP (S.A.)
Refinery A	328	323		326
Refinery B	370	413	246	406
Refinery C	134	135		134
Refinery D	152	161	101	160
Refinery E	38	48		42

ICP (Cal) – Results compared to NIST standards.
ICP (S.A.) – Results using standard additions.

TABLE VII
ICP Results Using Gasoline Standards Compared to ASTM Methods

Sample	Certified Value (mg/kg)	D-2622 (mg/kg)	D-5453 [1] (mg/kg)	D-5453 [2] (mg/kg)	ICP (Gasoline STD)
Sample A		404	396	420	509
Sample B		18	15	15	17
Sample C		321	345	303	396
Sample D		207	212	172	217
Sample E		59	41	39	43
Sample F		321	335	311	393
Sample G		193	193	188	229
Sample H		197	191	186	220
Sample I		198	204	185	222
Sample J		52	50	49	50
Sample K	0	11	12	11	0
Sample L	500	509	521	533	457
Sample M	20	32	30	32	20
Sample N	350	356	359	398	325
Sample O	50	60	59	61	48
Sample P	200	208	212	238	196
Sample Q	50	59	53	52	47

kerosene-to-gasoline ratio at 9 to 1. This ensured us essentially a perfect matrix match. The results generally agreed with other ASTM methods (see Table VI).

For samples where the matrix is not well-defined, or one that is variable, the method of standard additions is the best way to perform the analysis. However, since this is a very time-consuming process, we wished to find a way to analyze the sample by comparison to a calibration curve.

Calibration Using Gasoline Standards

In the course of our research, we found that Analytical Services (Houston, TX USA) manufactures sulphur standards in gasoline. We obtained standards with concentrations ranging from 0 to 300 mg/kg. We then analyzed 17 samples, comparing them to the gasoline standards. Two other laboratories, using ASTM D-5453 and D-2622, analyzed the samples. The results of this analysis are shown in Table VII and Figure 4.

Evaluation of NIST 2724a and 2724b

To further evaluate our method, we decided to analyze SRM 2724a and SRM 2724b. These standards are used for calibration in most laboratories using ASTM D-2622 and D-5453. We evaluated these samples for a one-month period and obtained the following results:

For SRM 2724a (certified value 430.4 mg/kg S), we determined a value of 432 mg/kg ± 18 mg/kg. Due to a limited amount of sample, only four replicates were measured.

For SRM 2724b (certified value 428.2 mg/kg S), we determined a value of 436 mg/kg ± 6 mg/kg. Standard deviations are given at 95% confidence limits.

CONCLUSION

This study shows that ICP is an accurate and precise method to measure the sulphur content in unleaded gasoline. However, one must exercise great caution with regard to instrument calibration and plasma parameter adjustments. Best results were obtained using sulphur standards prepared in gasoline. Comparison to ASTM methods shows that the ICP technique outperforms XRF (ASTM D-2622) at all concentration levels and is at least equivalent to UV fluorescence (ASTM D-5453) at all concentration levels, except for 0 to 10 mg/kg.

Received October 31, 2000.

REFERENCES

1. Lora Galvin, Sulphur in Gasoline: A Learning Module, Diploma Program in Enviromental Health, McMaster Institute of Enviroment and Health (MIEH), EcoResearch Chair's Program in Enviroment and Health, Hamilton (1999).
2. Karen Kohl, Rene Gonzalez, ASTM D 5453 Fitness for Use Study, Southwest Research Institute and World Refining (1999).

Determination of Wear Metals in Lubricating Oils Using Flow Injection AAS

Gustavo Pignalosa and Moisés Knochen*
Universidad de la República, Facultad de Química
Departamento Estrella Campos, Cátedra de Análisis Instrumental
Av. Gral. Flores 2124, Casilla 1157, 11800 Montevideo, Uruguay

ABSTRACT

The feasibility of flow injection analysis (FIA) was explored for the determination of wear metals in used lubricating oil by atomic absorption spectrometry. The difficulty presented by the viscosity of the samples was overcome by injecting the oil sample with a lab-made motorized syringe into a stream of kerosene. In order to achieve a thorough mixing of the two streams, a specially packed reactor was designed. The stream carrying the diluted sample was then carried to an AA spectrometer. A computer-controlled system was developed for injection and data acquisition allowing partial automation of the process.

The influence of several parameters (sample and carrier flow rates, reactor length) was studied.

Copper and iron were chosen as model analytes. Calibration was performed with Conostan standards diluted with unused oil. The accuracy was evaluated by analyzing real oil samples for copper and iron in the range of 1 to 40 ppm. The results were compared with those obtained by AAS measurement with manual dilution, using the joint-confidence ellipse F-test for the regression straight-line. No significant differences were found at the 95% confidence level. Precision of the results was 2.6% (RSD).

The analytical frequency attained was 30 hour^{-1}, which could be doubled with some software modifications. The stability of the proposed system was demonstrated during a 60-minute test, finding no evidence of drift in either baseline or sensitivity.

INTRODUCTION

Testing for metals content in lubricating oils is one of the most important controls carried out in engines. Metals may originate from additives in the lubricating-oil formulation (1), wear and oxidation of engine parts during operation, and contamination.

Wear metals monitoring is a useful diagnostic tool to determine the existence of abnormal operation as in aircraft engines, which could lead to catastrophic failure. An unusually high level of a metal can often pinpoint the origin of abnormal wear, because of the different alloys used in the various engine parts. Depending on the engine and the goal of the analysis, metals such as iron, copper, chromium, lead, silver, and tin are usually determined.

On the other hand, the service life of lubricating oils is limited due to deterioration of their physicochemical properties; thus, the oils need to be replaced after some time. A preventive maintenance approach, based on the replacement of lubricating oil on a mileage basis would be very expensive for the large engines employed in ships, locomotives, trucks, or aircraft. Therefore, the application of predictive maintenance is preferred. Under this strategy of maintenance, the oil is replaced if the wear metals content is above certain limits. This approach is less expensive in terms of oil costs; however, the workload of the analytical laboratory is increased.

Among the techniques employed for the analysis for wear metals in lubricating oils are flame atomic absorption spectrometry (FAAS) (2,3), inductively coupled plasma optical emission spectrometry (ICP-OES) (3-6), and X-ray fluorescence spectroscopy (XRF) (7). Technical reports (8) have been published dealing in detail with the subject of the analysis of metals in lubricating oils and the various techniques available. FAAS is not favored by some workers for lubricating oil analysis due to the influence of the size of the suspended particles in the results. In addition, its lower sample throughput for multielement determinations when compared with ICP-OES has been criticized. However, it is widely used for routine monitoring, especially in smaller laboratories, which do not have a heavy workload. It has been pointed out (9) that a judicious selection of a few metals that can be measured by AAS can provide sufficient information about wear conditions in the engine. Thus, the disadvantage of a lower sample throughput with AAS analysis is partially overcome.

Lubricating oil samples cannot be handled directly by standard nebulizers used in ICP and atomic absorption (AA) spectrometers due to the high viscosity of the oils. Sample preparation procedures for analysis range from complete ashing, followed by dissolution in inorganic acids, to dissolution in organic solvents (10), and even the production of acid/oil/solvent emulsions (11-13). The handling of viscous samples is slow and cumbersome. Laboratory automation (14,15) seems desirable in this context. It can provide advantages such as less manual handling, higher analytical productivity, and

*Corresponding author.
e-mail: mknochen@bilbo.edu.uy

use of less glassware, with the additional advantage of reduced glassware cleaning. Thus, it is surprising that automation is not a usual procedure in lubricant laboratories. Only some degree of mechanization is employed in commercial equipment by using a peristaltic pump as a sample introduction device for nebulizers in ICP spectrometers.

We decided to evaluate the use of flow injection analysis (FIA) (16), coupled to atomic-absorption spectrometry (AAS), for the dilution and injection of the samples. Flow analysis, especially flow injection analysis, has been successfully applied to numerous areas of chemical analysis and seems particularly convenient because of its simplicity and low cost of setup when compared with other forms of automation such as robotics or dedicated analyzers. Coupling of FIA to AAS has been widely experienced and accepted (17,18). However, a thorough revision in the literature has shown that there are very few papers that deal with the use of FIA for lubricant analysis. For instance, in a paper by Granchi et al. (19), FIA is used for sample introduction to an ICP spectrometer, but the dilution itself is performed previously by a laboratory robot in a fashion similar to the usual manual procedure. Berndt et al. (20) employed an HHPN (hydraulic high-pressure nebulization) flame AAS system for the determination of several metals in lubricating oil samples. Sample injection was performed by means of injection valves fitted with loops. Unfortunately, no description was given with regard to sample loading into the loops. As discussed below, peristaltic pumps are not dependable in the handling of highly viscous samples such as lubricating oils, even for the simple task of loading a loop. Thus, it was decided to resort to another kind of liquid handling device.

This work explored the feasibility of syringe injection into a FIA system for the analysis of wear metals in lubricating oils by AAS. A computer-controlled flow injection system was designed and built for this purpose. The system, consisting of a lab-built motorized syringe injector for injecting the oil samples into a solvent stream, and a packed reactor designed for thorough mixing of the sample and carrier streams, was evaluated and compared with a previously established manual procedure.

EXPERIMENTAL

Spectrometry

Detection was carried out with a PerkinElmer (Norwalk, CT, USA) Model 380 atomic absorption spectrometer with a 10-cm burner for air-acetylene flame, operated with hollow cathode lamps (Photron, Narre Warren, Australia).

Measurements were made at the wavelengths of 324.7 nm (Cu) and 248.3 nm (Fe). The acetylene flow was reduced to compensate for the presence of the organic solvent.

The absorbance signal was recorded as a function of time in a Shimadzu (Kyoto, Japan) C-R6A recorder.

Continuous-flow System

The continuous-flow system (Figure 1) consisted of a peristaltic pump, a syringe injector, a mixing device, and a mixing reactor.

The solvent stream was pumped by a Dynamax RP-1 peristaltic pump (Rainin Instrument Co., Woburn, MA, USA) fitted with Viton® tubing.

Sample injection was carried out by means of a lab-made motorized syringe consisting of a 1-mL syringe (Hewlett-Packard, Palo Alto CA, USA) and three 3-way, 12-volt solenoid valves (model 225T031, NResearch, West Caldwell, NJ, USA). The syringe was driven by a stepper motor, and the injector was controlled from the computer.

The oil sample and solvent streams were mixed by a mixing device, lab-built in acrylic material and fitted with PTFE connectors (Omnifit, Cambridge, England), and a packed mixing reactor made of 2.48-mm ID PTFE tubing filled with small pieces of PTFE as discussed below. The mixed stream was then

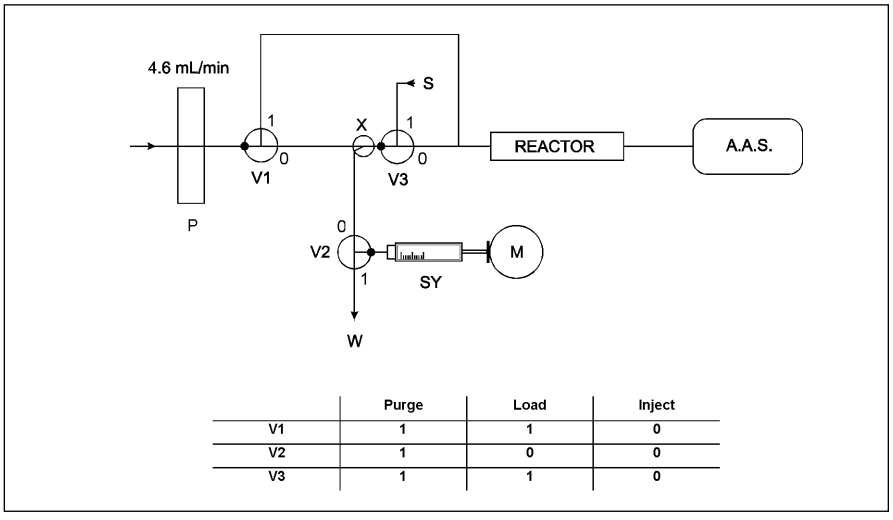

	Purge	Load	Inject
V1	1	1	0
V2	1	0	0
V3	1	1	0

Fig. 1. Flow diagram and valve activation table. P: peristaltic pump. X: Mixing device. S: Sample, V1, V2 and V3: Three-way solenoid valves. SY: Syringe. SM: Stepping motor. W: Waste. A.A.S.: Atomic absorption spectrometer.

carried to the nebulizer of the atomic absorption spectrometer.

All connections were made with 1.0-mm ID PTFE tubing and PTFE fittings (Omnifit).

Computer Control and Data Acquisition

An IBM®-compatible 80486-based 80-MHz personal computer running DOS 6.0 operating system (Microsoft®) was used for control and data acquisition. A multipurpose board (CIO-DAS-08AOH, ComputerBoards, Middleboro, MA, USA) was installed on the ISA bus of the computer. This card features a 12-bit analog to digital converter (ADC) as well as three counters, an on-board 1-MHz clock, and a number of digital inputs and outputs (I/O), which were used for logic control. Figure 2 shows the blocks diagram of the control and data acquisition system.

Data acquisition was carried out by means of the ADC, whose input was connected to the analog output of the spectrometer. Raw data were transformed to true absorbance through a scaling process. An optional subroutine allowed smoothing of the data by a 5-point moving average and finding peak height values, which were displayed on the screen. Unprocessed absorbance data were saved to the hard disk in ASCII format. The whole system was operated by means of a program in Quick-BASIC 4.0 (Microsoft) written for the purpose, which was linked to ComputerBoard's Universal Library, revision 3.4

Post-run processing of the ASCII files was achieved by means of a chromatography program (Peak Simple II, version 3.3, SRI Inc., Torrance CA, USA).

Reagents, Samples, and Standards

Deodorized kerosene (ANCAP, Montevideo, Uruguay) was used as

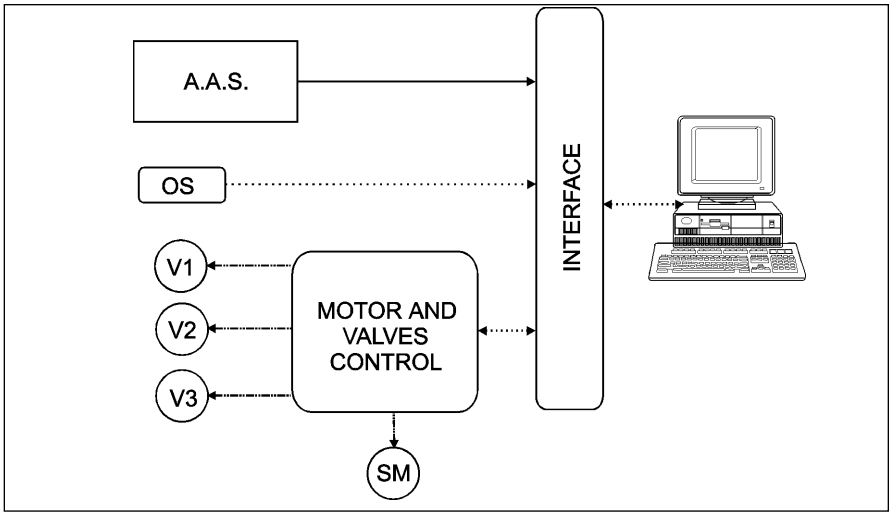

Fig. 2. Control and data acquisition diagram. A.A.S.: Atomic absorption spectrometer. OS: Optical switch. SM: Stepper motor. V1, V2 and V3: 12-volt three-way solenoid valves.
_____ Analog signal
..... Digital signal
- ·- ·· ·- ·· ·- ·· Power line

solvent and carrier. Conostan S-12 multielement 300-ppm standard (Conoco Specialty Products Inc., Ponca City, OK, USA) was used for calibrations and for preparing synthetic samples.

Unused SAE-40 Diesel lubricating oil (Superdiesel 40, ANCAP) was used as a blank and as diluent for preparing synthetic samples.

Real samples of used oil (Superdiesel 40, ANCAP) were taken from Alsthom locomotives belonging to AFE, a local railway company.

Standards and synthetic samples were prepared by mixing exactly weighed amounts of Conostan standard and unused oil.

Operation of the System

The syringe (SY) and three three-way solenoid valves (V1 to V3) were operated by the computer to route the oil samples appropriately as shown in Figure 1. The system performed three basic functions: load, inject, and purge. An additional verification function was implemented by means of an optical switch (OS), which is actuated when the syringe reaches the “full” position. This is designed to check that the syringe operates properly and to establish the zero position. In this phase, the valves are connected in "purge" position. When the system starts up, this routine is run automatically. At the end of this routine, the syringe is left at the "empty" position, which is taken as the reference (zero) position from which motor steps are counted. No feedback of the syringe’s motion was included in the operation of the system.

The valve setup was devised such that when the syringe is loaded, the sample passes through the mixing device and valve V2. In this way it is expected that the void volumes inside these components are swept with fresh sample, helping to reduce carryover from previous samples.

When changing samples, two purge operations are performed in order to purge the system with the new sample. Besides, one purge operation is carried out between injections of the same sample.

Reference Method

For comparing the results, a reference AAS method widely used in oil laboratory was employed. This reference method consisted of manual dilution (1 + 4 by mass) of the sample with kerosene and flame AAS measurement.

RESULTS AND DISCUSSION

Sample Injection

Lubricants are highly viscous. This poses a difficult challenge to the device used for sample injection, which should be capable of handling the sample in an accurate and reproducible way.

In the majority of modern FIA systems, injection is performed by means of some kind of injection valve fitted with a loop. Some means should then be provided for loading the loop. If the system is to be automated, one channel of a peristaltic pump should be used for this purpose. In this work, preliminary experiments showed that this approach was not convenient for lubricating oil samples. Peristaltic pumps do not perform appropriately with viscous samples such as lubricating oils, requiring long purge times between samples to avoid memory effects. Another drawback is the comparatively high dead volume of pump tubes, which requires an accordingly long time to be purged and filled with a new sample, increasing the amount of time required when the sample is changed. In theory this could be partly circumvented by making the sample pass first through the loop and then through the peristaltic pump. However, preliminary experiments showed that peristaltic pumps perform poorly as sippers when high viscosity samples are to be pumped.

To make things worse, viscosity varies widely between different oil types. It also varies with temperature and depends strongly on usage of the oil, because of polymerization of the oil and dilution with fuel during its service life.

In the early times of flow injection analysis, syringes were used for sample injection, but were soon abandoned due to the widespread use of sampling valves. Syringes however are dependable, easily motorized, and permit an easy variation of the injected volume, which results in added flexibility. In addition, the piston sweeps the fluid out of the barrel mechanically, thus minimizing carryover. Thus, it was decided to evaluate the use of a syringe as the injection device.

Performance of the injection device is critical for the present project. Hydrodynamic resistance of the oil should not cause the motor to lose control and the system should perform reproducibly, injection after injection. To ensure the accomplishment of this goal, the injector's motion was visually examined for step skipping. The motion was found to be smooth, with no indication that the motor might be losing control of the motion under the current set of conditions.

Characteristics of the Mixing Device and Mixing Reactor

Owing to the high sample viscosity, the mixture with the carrier solvent is difficult to obtain. With less viscous fluids, a good mixture can be obtained by using a "T" mixing device, but lubricating oils require the use of a more advanced mixing device and reactor. In previous experiments, several designs were evaluated for both the mixing device and mixing reactor.

The mixing device was lab-made out of Perspex® material, where two channels (internal diameter ca. 1 mm) were drilled. In preliminary experiments, the effect of the angle formed by the two channels was studied. With some designs, memory effects were found due to the presence of dead volumes. Best performance was obtained with a mixing piece where the sample channel meets the carrier channel at an angle of 30º.

As for the mixing reactor, best results were obtained in previous experiments with a tubular reactor packed with small pieces of the same tubing. Thus, it was decided to use this kind of reactor. The reactor was made out of a length of PTFE tubing (2.48 mm ID, 4.0 mm OD). From the stock tubing, thin slices (around 1 mm thickness) were cut. Each slice was in turn divided into four quarters. These small pieces were carefully inserted into the tubing and served as packing. The random nature of the packing forces the liquid streams into flowing in complex patterns with multiple direction changes, ensuring a thorough mixing of oil and solvent.

Performance of the packed reactor was evaluated both visually and analytically. Visually, by injecting unused oil samples containing a dye and observing the mixing pattern with a magnifying glass, and analytically by operating the system with oil standards and observing the signal shape and height.

The influence of the reactor length was studied by preparing reactors of 4, 6, 8, and 10 cm. According to peak shapes and heights, 6 cm was deemed an appropriate length, as 4 cm produced an incomplete mixture and longer reactors gave lower analytical frequency and peak height with no advantage.

Flow Rates

In a hyphenated system such as described, the range of total flow rates is limited by the characteristics of the detector used, in this instance by the nebulizer of the AAS spectrometer. There is an optimum intake rate that will provide the highest sensitivity.

A real sample of used lubricating oil (containing 6.35 ppm copper, determined by the reference method described above) was analyzed for copper at 324.7 nm. Kerosene and sample flow rates were varied to assess their influence on response (sample peak height minus blank peak height) and peak shape. The injected sample volume and the reactor length were kept constant at 200 µL and 6 cm, respectively. Solvent flow rate values were 3.8, 4.6 and 5.4 mL min^{-1}, while sample flow rates were 1.2 and 2.4 mL min^{-1} (see Figure 3). A sample flow rate of 2.4 mL min^{-1} showed increased sensitivity when compared with 1.2 mL min^{-1}. In the variation of the kerosene flow rate, no advantage was found beyond 4.6 mL min^{-1}. Therefore, a kerosene flow rate of 4.6 mL min^{-1} and a sample flow-rate of 2.4 mL min^{-1} were chosen.

The viscous nature of the sample does not allow fast motion of the syringe's plunger; thus, the motor speed was kept low to avoid splitting the syringe's barrel or the motor losing control of the motion. For this reason, sample flow rates higher than 2.4 mL min^{-1} could not be used with this particular syringe.

Peak Shapes

During injection of the oil sample (100-200 µL at 2.4 mL min^{-1}), the total flow rate is changed significantly, from 4.6 mL min^{-1} to 7.0 mL min^{-1}, and then back to 4.6 mL min^{-1}. Thus, it was important to determine whether this could affect peak shape. Under careful inspection, no evidence of peak deformation was found when using the flow rates of 4.6 mL min^{-1} (carrier) and 2.4 mL min^{-1} (sample injection).

The transient perturbation of flow change does not affect peak shape, because the injection finishes before the sample bolus reaches the nebulizer and the flow is constant during data acquisition. Thus, peak shape does not differ significantly from that of a usual FIA peak.

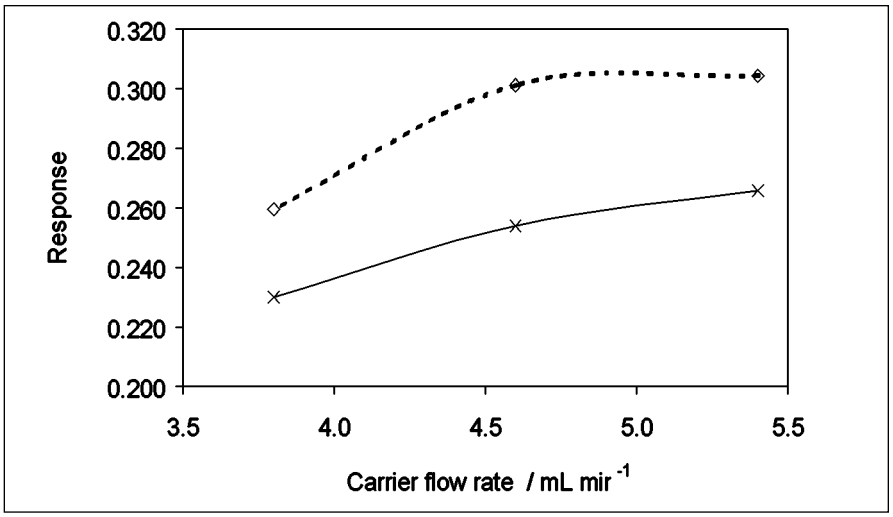

Fig. 3. Influence of carrier and sample flow rates on system response (sample peak height minus blank peak height, absorbance). Real used oil sample, containing 6.35 ppm copper (determined by reference method). Model analyte: copper, λ = 324.7 nm. Sample volume: 200 µL. Reactor length: 6 cm.

x *Sample flow rate 1.2 mL* min^{-1}
◆ *Sample flow rate 2.4 mL* min^{-1}

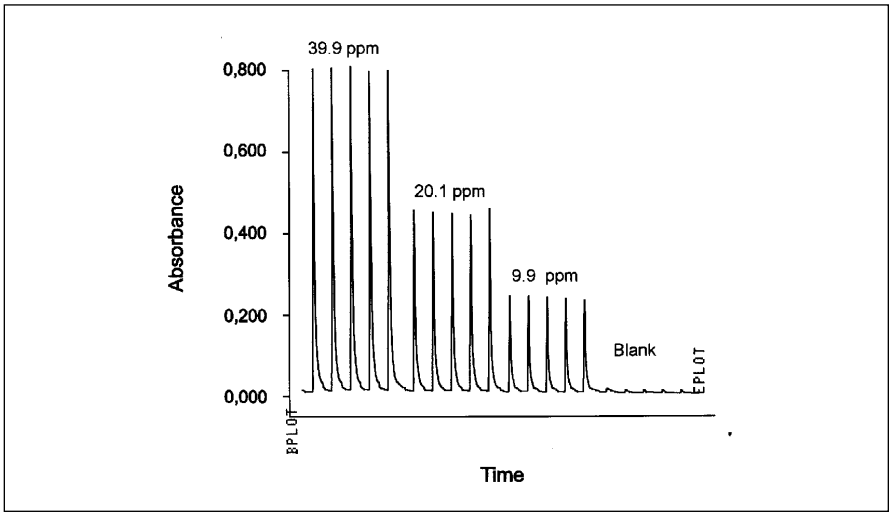

Fig. 4. Recorder output for a copper calibration curve (9.9, 20.1, 39.9 ppm and blank).

Linearity

Calibration curves (peak height vs. concentration) in the range of 0 - 40 ppm were fitted by the method of least squares (Figure 4). In each instance, the best model was chosen by means of the LOF (lack-of-fit) statistical test. At a confidence level of 95%, a second-degree polynomial was usually found the best-fitting model.

Atomic Spectroscopy
Vol. 22(1), January/February 2001

Accuracy and Precision

The proposed system is a sample handling device, coupled to a detector based on a well-known AAS technique. AAS is routinely used in batch fashion for the same analytical purpose. Thus, it was decided to evaluate accuracy by comparison of the flow method versus the batch method. No effort was undertaken to assess the accuracy of AAS itself as an analytical technique, because this was beyond the scope of this work, and AAS is widely used for oil analysis as stated before. On the other hand, in the batch method the dilution is made by mass, while the flow system performs the dilution by volume. Therefore, it was important to evaluate whether the proposed system could produce results that would not differ significantly from the well-established batch AAS method.

Accuracy was evaluated analyzing ten used-oil samples (containing copper and iron in the range of 1 - 40 ppm) by two methods, i.e., the proposed flow method and the reference method described before. For the two metals determined (copper and iron), the results obtained by the flow system were plotted against those obtained by the reference method by means of linear regression. Slope and intercept of the straight line obtained were compared with the theoretical values of 1 and 0 by means of the joint-confidence ellipse F-test (21). Table I shows the statistical tests and the results obtained.

At the confidence level of 95%, no evidence of a difference was found between the results obtained by the proposed system and those obtained by the reference method. This is consistent with the fact that both methods are based on the same analytical technique (AAS); therefore no difference is to be expected as long as the dilution is performed appropriately by the system.

TABLE I
Joint-confidence Ellipse F-test for the Regression Straight-line Obtained for Copper and Iron[a]

Parameter	Copper	Iron
a_{exp}	0.973	1.002
b_{exp}	0.193	-0.383
F_{exp}	2.31	2.11
Result	Pass	Pass

[a]Results from flow method plotted against results from reference method, $x_1 = ax_2 + b$). H_0: a = 1 and b = 0. H_A: a ≠ 1 and/or b ≠ 0. $F_{0.05}$ (2,8) = 4.256, n = 10.

Precision of the flow system, as measured by the relative standard deviation, is slightly poorer than that obtained by the conventional batch method. Average RSD values of 2.6% (n = 5) were found, which is acceptable for routine controls. It is believed that enhancing the volumetric resolution of the syringe could contribute to a lower dispersion of the results.

Solvent Consumption

Based on the carrier solvent operating flow rate, solvent consumption was estimated at 5 mL per determination. This consumption is lower than that of the conventional batch method, which is usually about 25 mL per determination.

Stability

The main factors affecting stability of the results are the injection system itself, the mixing reactor, and the spectrometer. Stability was assessed by repeatedly injecting a synthetic oil sample (containing 20.1 ppm of copper) over a period of 60 minutes and monitoring the response at 324.7 nm. No significant drift was found in baseline or sensitivity, as shown in Figure 5.

Carryover

When analyzing viscous samples, carryover between samples is of major concern. In order to help reduce carryover in this system, dead volumes were minimized, and a special flow configuration was devised for loading the syringe. In

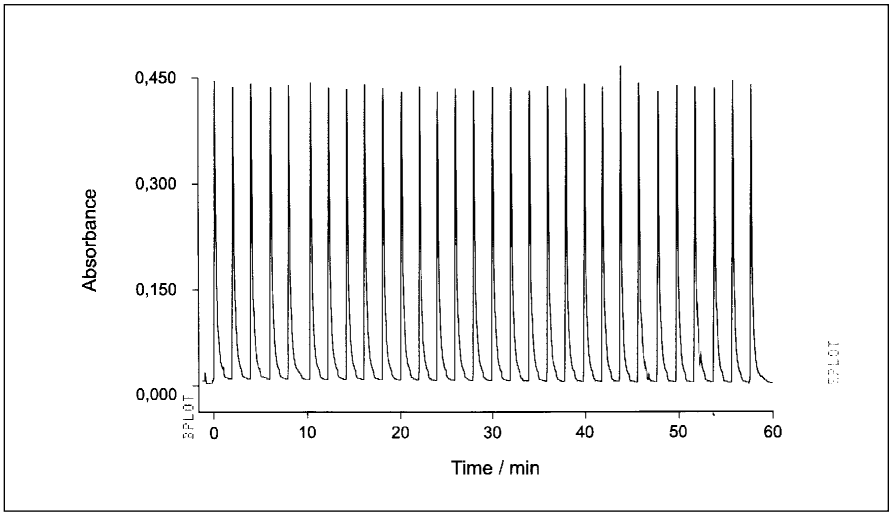

Fig. 5. Recorder output for a 60-minute stability test. Sample: synthetic sample containing 20.1 ppm copper. λ *= 324.7 nm.*

this system, the samples are loaded "backwards" traversing the solenoid valve and part of the mixing piece, thus helping sweep out any residue of previous injections. Besides, a number of purges were programmed between injections. In either case, the number of purges can be easily programmed. As a matter of compromise between minimum carryover and maximum analytical frequency, two purges between injections were chosen.

In order to assess the amount of this effect, five injections of a 20.1-ppm copper standard solution (Conostan standard diluted with oil base) were made, followed by five blank injections. The results are shown in Figure 6. When all measurements are corrected for the blank, carryover is about 2% for the first injection of base oil blank made immediately after the copper solution, and is negligible for the second and following injections. The reverse change (blank injection followed by injection of a 20.1-ppm solution) showed no measurable carryover.

Blank injections always generate a small signal of about 0.007 absorbance. Based on our experience, this is not due to contamination by metals but rather due to slight changes in the flame characteristics when base oil is burned in the flame mixed with the carrier solvent.

It was concluded that with this configuration and the selected number of purges, no significant carryover exists when samples with large differences in concentration are injected concomitantly. The main drawback is a low analytical frequency, which could be enhanced by a different software approach as discussed below.

Analytical Frequency

The analytical frequency was determined mainly by the syringe operation (purge, load, and inject times), the residence time of the sample bolus in the mixing reactor and tubing, and the measurement time.

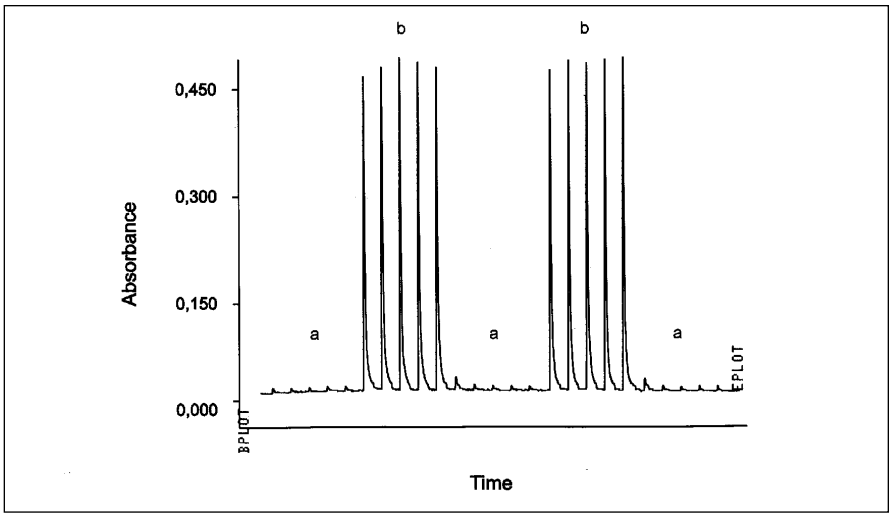

Fig. 6. Recorder output of carryover study. (a) Base oil blank and (b) 20.1-ppm Cu in base oil.

Under the selected operating conditions, the analytical frequency was about 30 hour^{-1}, which may seem low. In this work, no further effort was carried out to enhance this parameter; however, this could easily be done using multitasking software. The analytical frequency is not only a consequence of the flow process, but also of the time dedicated to the capture of the FIA peak, which is about one half of the total time. Since the current program cannot perform two tasks simultaneously, it is necessary to wait for the signal to return to baseline before the next actions (purge, load) are performed. Thus, with a multitasking program, the analytical frequency could be almost doubled since purging and loading of the next sample could be performed while the previous peak is eluting.

CONCLUSION

The feasibility of the FIA-AAS approach was established as a low-cost automation tool in the routine lubricating oil laboratory. Stability, precision, and accuracy obtained were found appropriate for routine monitoring of the concentration of wear metals in oil samples. Among the advantages offered are low solvent consumption, less pollution, reduced glassware usage, and a considerable reduction in time devoted to glassware cleaning. It is considered that performance of this prototype is promising and deserves further development, which is currently being carried out in our laboratory.

ACKNOWLEDGMENTS

The authors thank Luis Mussio and Alvaro Gancharov for their valuable help in the construction of the motorized syringe and electronic system, Isabel Dol for helpful discussion of statistical tests, and Administración de Ferrocarriles del Estado (AFE) for providing the used oil samples.

Partial financial support from UNDP/PEDECIBA (Program URU/97/016) is gratefully acknowledged.

Received November 27, 2000.

REFERENCES

1. T.V. Liston, Lubrication Engineering 48, 389 (1992).
2. 1992 Book of ASTM Standards, Section 5, V. 5.03, American Society for Testing and Materials, Philadelphia, PA USA, Method D -4628-86 (1992).
3. 1992 Book of ASTM Standards, Section 5, V. 5.03, American Society for Testing and Materials, Philadelphia, PA USA, Method D - 5184-91 (1992).
4. 1992 Book of ASTM Standards, Section 5, V. 5.03, American Society for Testing and Materials, Philadelphia, PA USA, Method D - 5185-91 (1992).
5. P.N. Bangroo, C.R. Jagga, H.C. Arora and G.N. Rao, At. Spectrosc. 16, 118 (1995).
6. C. Anderau, K.J. Fredeen, M. Thomsen, and D.A. Yates, At. Spectrosc. 16, 79 (1995).
7. 1992 Book of ASTM Standards, Section 5, V. 5.03, American Society for Testing and Materials, Philadelphia, PA USA, Method D - 4927-89 (1992).
8. C.S. Saba, H.A. Smith, and R.E. Kauffman, Alternate Spectrometric Oil Analysis Techniques, Report UDR-TR-91-156, U.S. Department of Commerce, National Technical Information Service, Springfield, VA, U.S.A. (1992).
9. B. Welz and M. Sperling, Atomic Absorption Spectrometry, 3rd edition, Wiley-VCH, Weinheim, Germany, p. 720 (1999).
10. J.A. Burrows, J.C. Heerdt, and J.B. Willis, Anal. Chem. 37, 579 (1965).
11. A. Salvador, M. de la Guardia, and V. Berenguer, Talanta 30, 986 (1983).
12. M.P. Hernández, J.A. Muñoz, and R. Cozar, Analyst 117, 963 (1992).
13. I.M. Goncalvez, M. Murillo and A.M. González, Talanta 47 1033 (1998).
14. V. Cerdá and G. Ramis, An Introduction to Laboratory Automation, Wiley, New York (1990).
15. P. B. Stockwell, Automatic Chemical Analysis, Taylor and Francis, London, UK, 2nd edition (1996).
16. J. Ruzicka and E. Hansen, Flow Injection Analysis, Wiley, New York, 2nd. Edition (1988).
17. Flow Injection Atomic Spectroscopy, ed. J. L. Burguera, Dekker, New York (1989).
18. J.F. Tyson, Spectrochim. Acta Rev. 14, 169 (1991).
19. M. P. Granchi, J. A. Biggerstaff, L. J. Hilliard, and P. Grey, Spectrochim. Acta B 42, 169 (1987).
20. H. Berndt, G. Schaldach, and S.H. Kägler. Fresenius' J. Anal. Chem. 355, 37 (1996).
21. J. Mandel and F.J. Linnig, Anal. Chem. 29, 743 (1957).

Aerosol-Cooled Plasma for Use With Microwave-Induced Plasma Spectrometry

Henryk Matusiewicz
Politechnika Poznańska, Department of Analytical Chemistry
60-965 Poznan, Poland

ABSTRACT

A simple torch design for use with a microwave-induced plasma (MIP) is described that can be internally cooled by water aerosol. The MIP is generated within an aerosol-cooled quartz discharge torch, energized within a microwave plasma cavity. An inexpensive common room ultrasonic humidifier has been developed for the aerosol generation and circulation. Erosion of the discharge tube by the plasma, assessed by measurement of the emission intensity of ablated silicon and lithium, is essentially eliminated. The emission spectra and noise amplitude spectra of the aerosol-cooled plasmas are compared to those for the air-cooled discharge tubes commonly employed. Analytical performance of the system was characterized by the determination of the limits of detection for Ca, Cd, Fe and Zn and their comparison with other Ar-MIP systems using sample introduction in the form of a wet aerosol.

INTRODUCTION

Microwave-induced plasma (MIP) has been used for more than two decades in atomic emission spectrometry (AES). A crucial component of MIP is the torch, with the function to contain the plasma and permit mixing of sample streams with make-up gas when necessary. The most commonly used MIP torch consists of an open quartz capillary tube with typical dimensions of 5 to 8 mm o.d. and 0.5 to 3 mm i.d.. However, these are plagued with poor long-term stability resulting from tube degradation, erosion, etching and/or melting. Ceramic tubes (e.g., Al_2O_3, ZrO_2, SiC) show a longer lifetime but their resistance to erosion or thermal shock is also often limited. Other discharge tube materials, such as boron nitride, are also superior to quartz or ceramic, but it is difficult to sustain lower power plasmas in such tubes.

Some effort has been made to eliminate these shortcomings. Cooling of the torch (discharge open tube) with liquids seems to be an attractive solution to this problem. Several designs have been proposed and various liquids were reported as highly efficient cooling media, including water, transmission fluids, and silicon oils (1,2). Water cooling, although very efficient, has certain disadvantages. First, distilled water not only absorbs microwaves but it also must be a thin layer to reduce attenuation in the microwave cavity. Secondly, water, and generally any liquid that can serve as a very efficient cooling agent, is simply too efficient for this specific application. Such over-efficient cooling leads to an over-cooled torch, generally below 30ºC, resulting in excessive energy loss in the resonant cavity. A temperature above 30ºC would still be acceptable to prevent quartz tubes from melting and at the same time this hot environment can save an appreciable amount of plasma energy. Thirdly, there is the possibility of gas bubbles forming in the cooling water. When such bubbles form, water flow can be interrupted, resulting in torch devitrification or melting.

These disadvantages suggest reconsideration of the design of the cooling system. Aerosol cooling is less efficient due to a lower heat capacity. Fundamentally, microwaves do not couple efficiently to droplets; therefore, the aerosol drops are unable to absorb microwave radiation since they have a much smaller size (a few microns) than the wavelength used (cm). This preliminary investigation describes the implementation of an ultrasonic humidifier water aerosol generator for cooling of the open quartz discharge tube of a microwave cavity-sustained plasma. Attention is also given to practical aspects such as ignition and ease of operation. Recently, similar cooling systems have been successfully used for an aerosol-cooled torch in MIP-AES (3).

EXPERIMENTAL

Aerosol-cooled Plasma Torch

Apart from sustaining the microwave plasma, the main function of the MIP torch is to prevent the quartz tube from melting. The design of the torch used in this study is shown in Figure 1. A demountable construction is used (Plazmatronika Ltd., Wroclaw, Poland) and consists of two tubes. A larger diameter ceramic tube (made of dielectric material, 15 mm o.d. and 13 mm i.d.) acts as a jacket around the inner quartz discharge tube and consists of an inlet and outlet for the cooling agent. The inner tube (plasma torch discharge tube, 6.0 mm o.d. and 3.0 mm i.d.) was made of transparent quartz. The two tubes are concentrically positioned. A flow channel of the cooling medium is formed between the external surface of the torch and the internal surface of the ceramic tube. Aerosol is channeled along the central sleeve of the resonant cavity body into the annular interspace between the torch and the jacket tube, and then exits through the front assembly. Viton® O-rings ensure water-tight seals

*Corresponding author.

Atomic Spectroscopy
Vol. 22(1), January/February 2001

between the quartz torch and the ceramic tube and the appropriate surfaces of the body cavity and back and front assembly. The inlet and outlet ports are on opposite sides of the two perpendicular partitioning walls of the cavity. The temperature of both the inlet and outlet ports of the cooling agent was measured by means of a NiCr thermocouple and ranged from 20 to 120ºC.

Aerosol-generated Cooling System

The main components of the closed cooling interface are shown in Figure 2. A room ultrasonic humidifier unit, Model UH-100S (Poland) (power 14 W, 1.35 MHz), was used for cooling the plasma torch. A fan motor (rotary blower) circulates the aerosol through the cooled torch assembly. In the cooling circuit system, PVC tubes connect the inlet and outlet of the aerosol-cooled torch assembly. The coolant water aerosol circulates in and out of it. The outlet PVC tube serves as an aerosol-cooled condenser. Only distilled water aerosol was used as the cooling agent.

Instrumentation

The plasma system consisted of a 700 W, 2.45 GHz stabilized generator coupled to a TE_{101} rectangular cavity (Plazmatronika Ltd., Wroclaw, Poland). The microwave cavity and generator used have been previously described (4).

Gas flow rates were controlled and monitored with mass flow controllers (DHN, Warsaw, Poland) using a digital read-out. Argon was of high-purity grade.

A pneumatic concentric glass nebulizer (TR-30-A3, Meinhard Assoc., USA) with an ARL conical spray chamber was also used in these studies. A Minipuls™ 3 peristaltic pump (Gilson, France) was used to deliver the test solutions to

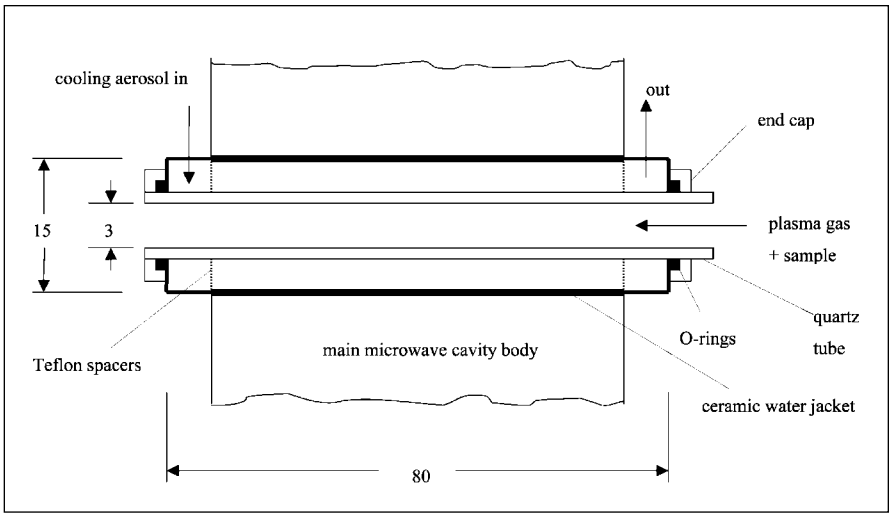

Fig. 1. Schematic diagram of the aerosol-cooled torch (all dimensions are in mm).

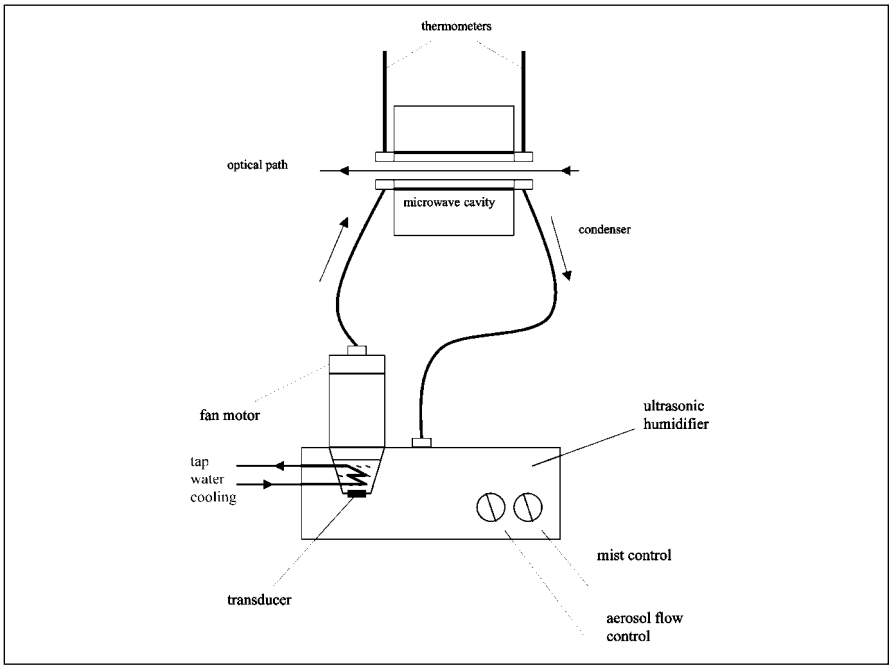

Fig. 2. Schematic diagram of the aerosol cooling system.

the nebulizer. A desolvation system was not employed in the introduction of aqueous samples. The standard solutions of the elements were prepared from BDH standard stock solutions (England). The water used was triple-distilled.

A 1:1 axial image of the plasma was focused onto the entrance slit of a computer-controlled echelle spectrometer (PLASMAQUANT 100, Carl Zeiss, Jena, Germany) described by Quillfeldt (5) and Matusiewicz (6,7). The position of observation was selected at the center of the plasma.

Procedure

Conversion between the air-cooled and aerosol-cooled plasma torch simply involved the installation of the appropriate ceramic jacket tube of the structure of the

cavity, appropriate plasma torch, and the front and back ports where necessary.

The plasma was allowed to equilibrate for 15 minutes prior to use. Simultaneously, cooling of the discharge tube torch was started. Silicon and lithium emissions were monitored from both the cooled and uncooled torch to provide an indication of the extent of plasma contact with the walls. Measurement of the Si 288.2-nm and Li 670.7-nm lines were performed under typical operating conditions (i.e., forward power 210 W, argon flow rate 1.0 L/min). The same data collection system and viewing geometries were used for both measurements.

RESULTS AND DISCUSSION

Operation of Aerosol-cooled System

The argon plasma is easily ignited within either the uncooled or cooled torch by momentarily inserting a short length of tungsten wire mounted on an appropriately insulated handle. An ultrasonic humidifier, pump fan, and outlet tube condenser are used in a closed cooling system. During typical MIP cavity operation, the water aerosol quickly converts into an overheating steam, expanding from the quartz tube surface. After passing through a condenser, it becomes water again, additionally cooled inside the humidifier by a secondary tap water cooling. When it is exposed to the ultrasonic transducer, clouds of newly generated aerosol are sent back to the MIP cooling system by means of a rotary blower. Not only is minimal effort required when converting from an uncooled to cooled mode of operation, but also when altering either the applied power or plasma gas flow rates. The aerosol generation rate is a function of the "mist-control" switch (input power of transducer) of the humidifier and the amount of aerosol delivered to the cooling system can be regulated. Importantly, the cooling aerosol temperature depends on the intensity of aerosol generation. The efficiency of cooling can be controlled by changing the air flow from 0 to 3 L min^{-1} and the amount of the water aerosol from 0 to 20 mg min^{-1}. When cooling of the torch begins, the wall temperature decreases and a remarkable decrease of orange emission from the quartz is observed. A comparison of the heat release for argon and helium MIPs was made by measuring the temperature of the aerosol at the discharge tube torch outlet for plasmas maintained at forward powers of 210, 280, and 350 W. Constant temperature in the cooling system was obtained after 5 – 6 min of plasma operation. With the argon plasma, the temperature of the aerosol went up to 50, 70, and 90ºC, respectively, and with a helium plasma up to 60, 90, and 110ºC, respectively (before igniting the plasmas, the coolant temperature was 22ºC). When the temperature of the water aerosol is controlled and the "mist-control" is at the lowest, intermediate, or maximum settings, the aerosol generation process is stable over a relatively long period of time (more than three hours), a duration well suited for fundamental research and application purposes. Aerosol cooling considerably reduced erosion/etching of the interior wall of the quartz discharge tube. With this new kind of cooling, only slight erosion/etching is detectable after about 20 hours of operation. The erosion/etching of the uncooled tube reduced the discharge tube torch lifetime from minutes to hours (the degree of erosion/etching correlates directly with applied power level). Aerosol cooling of the torch eliminates these problems.

Background and Emission Characteristics

The first objective was to characterize the effect of water aerosol cooling on the observed background levels. The background emission spectrum between 200 and 700 nm was recorded. Erosion of the uncooled discharge tube leads to the presence of high background levels of major components of the tube material as well as contaminants in the discharge. The spectral background emission with an aerosol-cooled discharge tube torch was considerably reduced compared to the emission of an MIP operated in an uncooled (air-cooled) tube for several elements. Calcium, Cd, Fe, and Zn exhibit background intensities 2 – 3 times lower than in the uncooled system. Little background is observed for the aerosol-cooled plasma. The background emission levels of these elements are lower, because the inside wall of the discharge tube in the MIP cavity is much lower in temperature with aerosol cooling. It should be noted that the surface temperature in the region of the He plasma (210 W) wall contact is presumably above the melting point of quartz, because extended operation of the plasma resulted in a distortion of the tube when the torch was not cooled by flowing aerosol.

In the present study, Si and Li emissions at the 288.2-nm and 670.7-nm lines, respectively, were monitored during operation of both argon and helium plasmas contained in the uncooled and cooled torch. Presence of the Si line (288.2.nm) as well as presence of an emission line at 670.7 nm due to lithium, a common impurity in quartz, is visible in the spectrum of the uncooled (air-cooled) discharge tube torch in comparison to the spectrum for the water aerosol-cooled torch.

The influence of the cooling agent temperature on the intensity of the signal-to-background ratio (S/B) of the silicon and lithium lines was also investigated. A series of experiments was performed where the S/B of these elements was observed as a function of cooling temperature (between 30 and 110ºC). In general, for the Si and Li lines, a signal enhancement with increasing cooling temperature was observed. The intensities of spectral lines increases as the cooling temperature is raised from 70 to 110ºC. The S/B also increases, but more slowly. It would appear that in the temperature range studied (30 – 70ºC), small temperature differences do not have a noticeable effect on the background and signal intensities; in other words, the signals below 70ºC remain relatively constant. The other important information obtained from this temperature study was how quickly the background and signal intensities increase with cooling temperatures above 70ºC. This means that the use of a cooling temperature higher than 70ºC may result in better limits of detection and that the effect of temperature of the discharge tube wall on spectrometric determinations is significant. Why the intensities above 70ºC sharply increase is still unclear. It is believed that the cooling temperature is such that there is a threshold temperature where ablation of the inner torch wall begins. This new kind of cooling assures that the quartz discharge tube torch temperature does not exceed 70ºC, i.e., the temperature level measured at the steam outlet.

Detection Limits

Although the optimum operating conditions were not extensively examined, the detection limits (DLs) of four elements were measured under compromise experimental conditions by using a polychromator. The results were compared with those of the conventional quartz tube torch. The operating conditions for both torches are matched as closely as possible.

TABLE I
Comparison of Detection Limits (ng mL^{-1}) for the Water Aerosol-cooled Torch (WACT) and Uncooled Torch (UT) Obtained from Optical Emission Ar-MIP[a]

Element	Wavelength (nm)	LOD[b]	
		WACT	UT
Ca II	393.37	10	30
Cd II	226.50	90	200
Fe II	259.94	100	350
Zn I	213.86	80	220

[a]Applied power 210 W, Ar flow rate 1.0 L min^{-1}

[b]Limit of detection (3σ)

The calculated DLs observed with the present cooling system are listed in Table I, according to the 3σ criterion and are based on 10 blank records. The results obtained were compared with those of a similar experimental system (using an argon plasma and uncooled torch). Generally speaking, the detection limits observed with the water aerosol-cooled torch are superior to those obtained for the uncooled torch by a factor of 2 to 3. This is due to the lower background and hence higher S/B in the water aerosol-cooled torch.

The linear dynamic ranges for the elements investigated were two to three orders of magnitude.

CONCLUSION

The practicability of using a water aerosol-cooled torch for MIP has been demonstrated. The aerosol-cooled quartz torch described in this study is easily fabricated and can be used with a conventional MIP system without modification of the cavity and/or nebulizer. A common ultrasonic room humidifier was converted to a low-cost cooling system, operated in the continuous mode. Water aerosol evaluated in this study shows negligible absorption of microwave energy. It is assumed that the aerosol loss onto the walls of the quartz-ceramic channel, which is located inside the microwave cavity, results from electrical charging of the aerosol droplets. This charging is the result of thermal explosion rather than interaction of the aerosol droplets with the microwave energy. In practice, the cooling temperature of the torch can be controlled and fixed at specific temperatures by regulating the mist flow; therefore, application of water aerosol permits efficient and easily controllable plasma cooling. The application of cooling by means of water aerosol does not require the use of a torch of sophisticated design (1), as in the case of liquid media (1,2). Additionally, the aerosol cooling technique does not leave residues (carbonaceous deposition) on the quartz tube walls upstream from the plasma, and thus largely avoids memory effects. The aerosol-cooled torch enhances discharge tube lifetime and significantly decreases erosion/ablation of the quartz tube surface, leading to a background emission spectrum that is comparatively free of Si and Li lines. The water aerosol cooling provides some gains in signal intensity for the elements studied. In general, an overall gain is achieved due to improved signal-to-background ratios as a result of reduced back-

ground continuum. As a result, better detection limits were obtained. However, optimization of the detection limits has not been attempted.

A minor disadvantage is that cracks in the ceramic jacket tube were noticed (after about 50 hours of operation) that eventually lead to tube rupture. Perhaps use of more rigid quartz jacket tubes might prove effective and should be implemented for possible use in future designs.

ACKNOWLEDGMENT

Financial support by the State Committee for Scientific Research (KBN), Poland, Grant No. 3 T09A 061 10, is gratefully acknowledged.

Received June 19, 2000.

REFERENCES

1. H. Matusiewicz and R.E. Sturgeon, Spectrochim. Acta, Part B 48, 515 (1993).
2. J. Mierzwa, R. Brandt, J.A.C. Broekaert, P. Tschöpel ,and G. Tölg, Spectrochim. Acta, Part B 51, 117 (1996).
3. H. Matusiewicz, Spectrochim. Acta, Part B 47, 1221 (1992).
4. K. Jankowski, R. Parosa, A. Ramsza. and E. Reszke, Spectrochim. Acta, Part B 54, 515 (1999).
5. W. Quillfeldt, Fresenius' J. Anal. Chem. 340, 459 (1991).
6. H. Matusiewicz, Chem. Anal. (Warsaw), 40, 667 (1995).
7. H. Matusiewicz, Fresenius' J. Anal. Chem., 355, 623 (1996).

Determination of Gold in Rocks, Ores, and Other Geological Materials by Atomic Absorption Techniques

S.L. Ramesh, P.V. Sunder Raju, K.V. Anjaiah, Ramavathi Mathur, T. Gnaneswara Rao, B. Dasaram, S. Nirmal Charan, D.V. Subba Rao, D.S. Sarma, M. Ram Mohan, and V. Balaram*
National Geophysical Research Institute
Hyderabad - 500 007, India

ABSTRACT

A method was designed for the determination of gold in geological samples such as rocks, ores, and soils by flame atomic absorption spectrometry (FAAS) and graphite furnace atomic absorption spectrometry (GFAAS) with Zeeman background correction. Ten grams of each sample was decomposed with aqua regia after heating at 650ºC. Gold was extracted into methyl iso-butyl ketone (MIBK), which was then analyzed by AAS after removal of the interfering iron from the organic phase. FAAS was used for the determination of gold up to a concentration level of 0.1 µg/g. The results obtained by FAAS compared favorably with those obtained by the fire assay and ICP-MS methods. In the lower range of gold concentration, agreement between the values obtained by GFAAS and ICP-MS is also appreciable.

For verification of the efficacy of these methods, international gold standard reference materials were utilized.

The results obtained in this study demonstrate that reliable results suitable for use in geochemical prospecting of gold can be obtained with a sample weight of 10 g, using aqua regia digestion and MIBK extraction, followed by the AAS determination of gold.

INTRODUCTION

The determination of gold in geological samples is a challenging task in view of its (a) availability in nature in varied concentrations, (b) heterogeneous distribution, (c) nugget-like mode of occurrence, and (d) high economic value (1). The increase in gold exploration has led to further development and refinement of methodologies for the determination of gold in rocks, ores, and other geological materials (2). The very low average concentration of 4 ng/g gold in rocks (3) requires highly sensitive analytical techniques for its quantitative estimation. Many techniques are available for the determination of gold using either the classical methods, such as fire assay (FA) (4) and cyanidation (5,6), or the modern instrumental methods such as flame atomic absorption spectrometry (FAAS) (7-9), graphite furnace atomic absorption spectrometry (GFAAS) (10), inductively coupled plasma atomic emission spectrometry (ICP-AES) (11), inductively coupled plasma mass spectrometry (ICP-MS) (12,13), and instrumental neutron activation analysis (INAA) (14). Very often these techniques are coupled with pre-concentration methods, such as solvent extraction, ion exchange, or coprecipitation. Although the classical fire assay technique has achieved confidence of use in the mining laboratories, use of the instrumental analytical techniques, particularly FAAS, has proved to be most cost-effective.

FAAS gives reliable results when combined with a solvent extraction procedure for the separation of gold even from a rock matrix, which is rich in the interfering species of iron, present in appreciable quantity in sulfide faces banded iron formations (SBIF). Distribution of gold in most geological samples is not homogeneous. It occurs either as grains of native gold or an alloy of gold, silver, and copper, or often as tellurides associated with base metal sulfides and other minerals. Hence, it is important that a representative sample is chosen for analysis. For digestion, a relatively large amount of sample is required to obtain reliable values. Small sample amounts generally lead to inaccurate estimation of gold (1).

This paper evaluates the following parameters:

(a) A procedure designed for the estimation of gold in rocks, ores, and soils by FAAS and GFAAS with Zeeman background correction, after methyl iso-butyl ketone (MIBK) extraction of gold.

(b) The reliability of the results using aqua regia leach-MIBK extraction, followed by FAAS determination of gold and comparison of the results with the fire assay method.

(c) The results from FAAS and GFAAS are compared with the ICP-MS method.

(d) Discussion will also focus on sample reduction, heating, sample decomposition, and solvent extraction for the quantitative recovery of gold and total removal of iron interference before gold is determined by FAAS and GFAAS.

(e) This publication is also intended as a status report on the analytical methods used for gold estimation in exploration studies in India and abroad, carried out at the Geochemical Laboratory of the National Geophysical Research Institute of Hyderabad, India.

EXPERIMENTAL

Instrumentation

For this study, a Model SpectrAA 220 flame atomic absorption spectrometer and a Model SpectrAA 880Z was used, equipped with a GTA-100 (Varian, Australia) graphite furnace atomic absorption

*Corresponding author.

spectrometer with Zeeman background correction. Details of the instruments are given elsewhere (15). The instrumental parameters (Table I) were optimized for maximum absorbance and the readings were taken between 0.1 to 0.4 absorbance. A Model Z300 benchtop centrifuge (Hermle Labor Technik, Germany) was employed for centrifuging the sample solutions.

Fire Assay Analysis

The fire assay (FA) analysis was carried out on 50-g samples at the Chemical Laboratory of Hutti Gold Mines, Karnataka, using the procedure proposed by VanLoon and Barefoot (4). The gold specks were weighed using a Model UMT2 microbalance (Mettler, Switzerland).

International Gold Reference Materials

Rock and ore standard reference samples having certified values for gold were obtained from various international agencies (Table II).

ICP-MS Analysis

The ICP-MS analysis was carried out using a PlasmaQuad PQ 1 (VG Elemental, UK). Five grams of each sample was dissolved using aqua regia, bromine, HF, and $HClO_4$. ^{103}Rh was used as an internal standard. The samples and standards were diluted using double-distilled water to 0.2% before analysis. More details are given in the literature by Balaram and Anjaiah (12).

Reagents

The acids and other reagents used were of EXCELAR™ grade. Fresh aqua regia was prepared before each experiment, using a 1:3 mixture of concentrated HNO_3 and HCl. Double-distilled water was used throughout. MIBK was distilled before use. The wash solution was prepared by adding 10 mL concentrated HCl and 10 mL concentrated HBr into a 500-mL volumetric flask. This solution was brought to volume with double-

TABLE I
Instrumental Parameters for Flame AAS

Wavelength	242.8 nm	Air flow	3.5 L/min
Lamp current	4.0 mA	Acetylene flow	1.5 L/min
Background correction	Using deuterium lamp	Burner height	12.5 mm
Flame type	Air - acetylene	Measurement time	5 sec

TABLE II
Details of International Gold Reference Materials[a]

Sample	Sample Type	Sources
GAu 8	Medium grained biotite granite	Institute of Geophysical and Geochemical Exploration, Langfang, Hebei 102849, China
GAu 9	Deluvia soil derived from granite	" "
GAu 10	Soil from a Carlin-type gold ore district	" "
GAu 11	Stream sediment from an epithermal auriferous sulfide mineralized ore district.	" "
GAu 12	Stream sediment from an epithermal auriferous sulfide mineralized ore district	" "
GAu 13	Soil with micrograined gold	" "
GAu 14	Soil from carbonate rock with micrograined gold	" "
GAu 15	Soil over auriferous polymetallic sulfide deposit	" "
GAu 16	Poor ore from altered sandstone gold deposit	" "
GAu 17	Ore from altered pelitic siltstone gold deposit	" "
GAu 18	Rich ore from hydrothermal metasomatic gold deposit in shattered fault belt	" "
Ox2	Sodium feldspar with minor quantities of gold bearing quartz	Rock Labs Ltd. Auckland, New Zealand
Ox4	Sodium feldspar with minor quntities of gold bearing quartz	" "
Ox5	Sodium feldspar with minor quntities of gold bearing quartz	" "
Ox8	Sodium feldspar with minor quntities of gold bearing quartz	" "
Ox9	Sodium feldspar with minor quantities of gold bearing quartz	" "
Ox11	Sodium feldspar with minor quantities of gold bearing quartz	" "
Ox12	Sodium feldspar with minor quantities of gold bearing quartz	" "
S 2	Sodium feldspar with minor quntities of gold bearing quartz and iron pyrites	" "
KH 1	Sodium feldspar with minor quantities of gold bearing quartz and iron pyrites	" "
WG 2	Siliceous oxidized gold ore containing finely disseminated gold	" "

[a] All other samples used in this study are field samples collected from Karnataka. These samples include sulfidic-banded iron formations, quartz veins, quartz-bearing volcanic rocks shaly sulfidic-banded iron formations and enriched ores.

distilled water. Gold calibration solutions of appropriate concentrations were prepared from a 1000-µg/mL stock solution obtained from Alfa Products, USA. An MIBK solution of 100-µg/mL Au was prepared by extracting gold from 100 mL of 100 µg/mL Au in 3M HCl in 100 mL MIBK in a 500-mL separating funnel. Calibration standards of 0.5 µg/mL, 1 µg/mL, 2 µg/mL, and 5 µg/mL were prepared from this stock solution and pure MIBK solvent for FAAS measurements. The calibration standards of 10 ng/mL, 20 ng/mL, 30 ng/mL, 40 ng/mL, and 50 ng/mL of gold were prepared using the automatic Programmable Sample Dispenser (PSD) by injecting varying volumes of 500 ng/mL gold in MIBK and pure solvent MIBK for GFAAS measurements. The calibration standards used in these investigations were found to be stable over a period of at least two months.

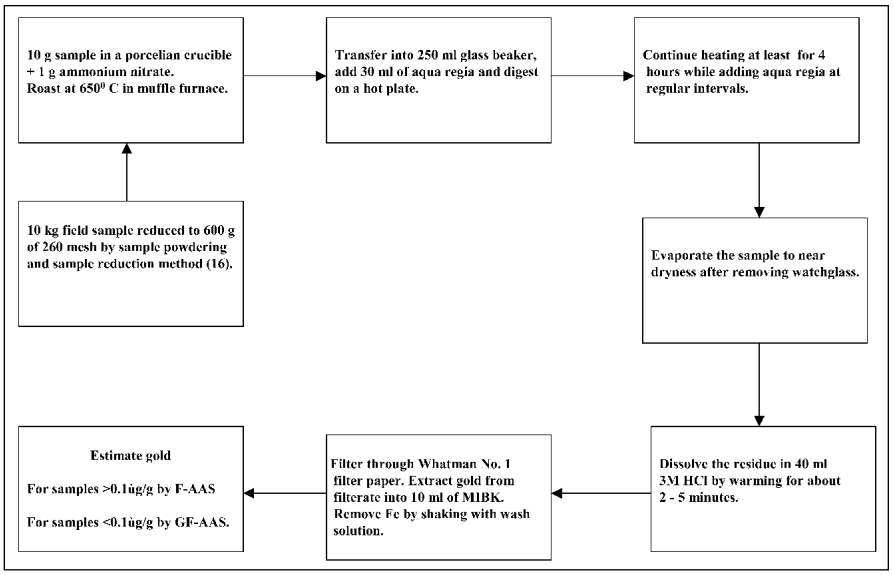

Fig. 1. Flow chart of the methodology used in the determination of gold in geological samples.

Geological Field Samples

Samples of 10 kg each were collected in the field and brought to the laboratory. Each bulk sample was reduced to 600 g of 260 mesh for chemical analysis, following the sample preparation flow chart described by Balaram et al. (16).

Laboratory Sampling Method

After powdering the samples to 260 mesh and homogenization, the sample powder was spread over an area of about 4 square feet on a polythene sheet to form a layer of uniform thickness. Square grids of approximately 2 square inches were made on this layer of sample using a clean plastic spatula. To obtain 10-g samples, small and uniform amounts of sample were scooped from each grid.

Sample Decomposition

Each 10-g sample was transferred into a porcelain crucible along with 1 g ammonium nitrate, then mixed thoroughly, and roasted for one hour in a muffle furnace at 650ºC. After roasting, the samples were transferred to 250-mL glass beakers and 30 mL freshly prepared aqua regia was added to each sample. One gram of NaCl was added to stabilize the gold chloride complex during evaporation on a hot plate (8). Each beaker was covered with a watch glass and heated on a hot plate. Heating was continued for at least four hours and enough aqua regia was added at regular intervals to maintain the free acid level at about one centimeter above the sample level. The watch glasses were then removed and the contents evaporated slowly until the residue became nearly dry. Then 40 mL of 3M HCl was added to each beaker and the solutions were warmed until clear solutions were obtained. These sample solutions were cooled and filtered using a Whatman No.1 filter paper. The residue was washed with minimum amounts of 3M HCl. The final residue was discarded and the filtrate used for the determination of gold.

Solvent Extraction of Gold

The filtrate of each sample was transferred to a 250-mL separating funnel. The beaker was washed with a minimum amount of 3M HCl and the washings were transferred to a separating funnel. Ten mL of MIBK (previously equilibrated with 3M HCl) was added to the separatory funnel and shaken for 5 minutes. After the phases were clearly separated, the aqueous phase was drained off. Then, a10-mL washing solution was added and the separating funnel shaken for two more minutes. After the phases were completely separated, the aqueous phase was discarded. The washing step was repeated to ensure total removal of iron. The organic phase was stored in 10-mL glass tubes with screw caps. The various steps involved in the sample reduction, sample decomposition, solvent extraction, and estimation of gold using different AAS methods are outlined in Figure 1.

AAS Measurements

The absorbance measurements were taken at the 242.8-nm line. The operating parameters (Tables I and III) were optimized to achieve maximum absorbance for gold in the working range. In the case of FAAS, the nebulizer spray chamber reservoir was filled with MIBK before starting the analysis. In the case of GFAAS analysis, Triton® X-100 solution was utilized for emulsification of the organic solution.

RESULTS AND DISCUSSION

Sample Weight for Analysis

To overcome problems associated with the heterogeneous distribution of gold in geological samples, 10 g of each sample was taken for analysis from a 10-kg field sample, 600 g sieved through 260 mesh. This sample amount is sufficiently representative for replicate analysis of different samples and provides reasonably consistent values. The famous graph of Clifton (17) also indicates that a sample of 5-20 g size is justified for gold analysis if the Au particle sizes are less than 4-6 µm. In addition, errors in sample preparation, sample decomposition, separation, and preconcentration contribute to the uncertainty of the results. In view of this, analysis of a single aliquot does not allow estimation of the possible uncertainties involved, particularly those caused while sampling. Therefore, replicate analyses were carried out to assess the reproducibility of the data. The analysis of certified reference materials (CRMs) helped to quantify the uncertainties in this investigation.

Sample Dissolution, Separation, and Preconcentration

Aqua regia ($HCl:HNO_3$, 3:1) and a mixture of bromine and hydrobromic acid are the two extraction systems that are generally adopted for the extraction of gold from rocks, ores, and other geological materials. Alkaline cyanide solution is another powerful medium for the extraction of gold (5,6). However, aqua regia leach is widely used for the determination of gold in geological samples. The success of the technique depends on the ability of aqua regia to dissolve native gold and its alloys associated with copper and silver. This property arises from the reactivity of nitrosyl chloride (NOCl) and the free chlorine formed in a freshly prepared aqua regia solution (18). Aqua regia attacks precious metals and also sulfides such as arsenopyrite, pyrite, and chalcopyrite, taking most metals into solution either as their simple chlorides or chloroanions. Chow and Beamish (19) have shown that when the samples are pre-roasted, an aqua regia attack is at least 99% efficient at removing gold from siliceous materials, such as gold-bearing quartz veins and quartz-bearing sulphides.

The sample decomposition method described by Rubeska et al. (8) was modified to suit this application. The samples were mixed with ammonium nitrate and roasted at 650ºC to remove the organic material and sulfide sulfur. The presence of ammonium nitrate makes the sample porous and facilitates oxidation of the sample for an effective extraction of gold into sample solutions when treated with aqua regia. After decomposition of the sample and after the excess acid was removed, the sample solution was not allowed to evaporate to dryness as gold may be reduced to a lower valence state and cannot be extracted. Extraction of Au(III) by MIBK from hydrochloric acid is the most common solvent extraction method adopted for the separation and pre-concentration of gold from geological samples (20). MIBK extraction is very efficient and the only possible interference is due to the high content of dissolved iron. This is particularly true with iron-rich samples such as BIFs (banded iron formations). In order to ensure total removal of iron, the organic phase should be washed twice with the wash solution and centrifuged (at 3500 rpm for 5 minutes) to remove even traces of the aqueous phase present before the determination of gold.

TABLE III
Operating Parameters of Graphite Furnace Atomic Absorption Spectrometer With Zeeman BGC

Atomization Program for the Estimation of Au		
Step	Temp (ºC)	Hold Time
Dry	85-120ºC	55.0 sec
Ash	120-800ºC	9.0 sec
Atomization	2600ºC	4.0 sec
Background correction	Zeeman	
Measurement	Peak height	
Argon flow	18 L/min	
Sample volume	20 µL	
Wavelength	242.8 nm	
Slit width	1.0 mm	
EHT	281 Volts	
Lamp current	4.0 mA	
Sampling mode	Automix	

FAAS and GFAAS Analysis

The optimum parameters for flame and GFAAS are shown in Tables I and II. The calibration curves for these two techniques are shown in Figure 2. The maximum ashing temperature of 800ºC was established without any loss of gold. The calibration graph was linear up to 55 ng/mL (Figure 2) with a sample injection volume of 10-20 µL. Gold concentrations obtained in a few field samples, in-house standards, and international geochemical reference materials using FAAS and GFAAS are given in Tables IV, V, and VI, respectively. Agreement between the values obtained and the certified values is reasonably good.

Comparison of FAAS and Fire Assay Values

For the determintation of gold in geological materials, the most popular and widely accepted method, particularly by the mining industry, is fire assay (FA). Normally large samples (15-50 g) are required for an assay after appropriate particle size reduction by crushing and grinding (4). The large weight of well-mixed samples used for FA analysis has the advantage of overcoming sampling errors caused by the nugget effect. The comparison results presented in Table VII for gold values obtained by FAAS and FA show that agreement between both methods is reasonably good.

Comparison of FAAS and GFAAS Values With ICP-MS Values

The advantage of ICP-MS in the determination of gold is its very high sensitivity coupled with extremely low background and limited interference effects. The pre concentration step can be avoided, providing a representative sample is taken for dissolution (12). Tables VII and VIII present comparative data on a set of field samples. The data obtained by both FAAS and GFAAS compare favorably with those obtained by ICP-MS.

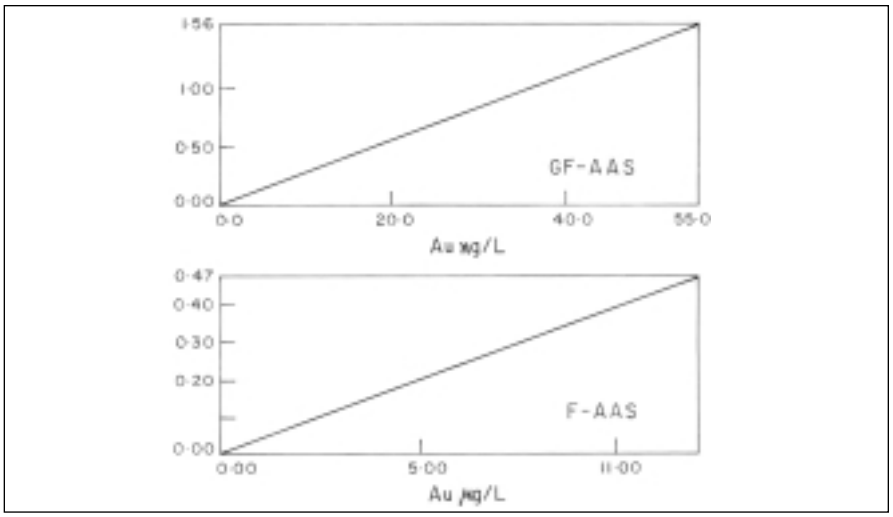

Fig. 2. Calibration curves obtained for gold in FAAS and GFAAS analysis.

TABLE IV
Gold Concentration (µg/g) in Reference Materials and Field Samples Using FAAS Analysis After MIBK Extraction in Comparison to Certified Values

Sample	Au (ug/g)	
	MIBK - FAAS Method	Certified Value (21)
HGX-1	2.85±0.31	
HGX-2	5.63±0.73	-
HGX-3	5.89±0.71	-
HGX-4	9.20±0.90	-
HGX-5	9.37±0.75	-
GAu-16	1.08±0.10	1.09±0.03
GAu-17	3.00±0.21	3.14±0.06
GAu-18	9.96±0.56	10.00±0.20
TKG-270	2.98±0.40	3.00±0.30

TABLE V
Gold Concentration (µg/g) in International Gold Reference Materials Using MIBK - FAAS Analysis in Comparison to Certified Values

Sample	Au (µg/g)	
	MIBK - FAAS Method	Certified Value [a]
Ox-2	1.40±0.08	1.42±0.02
Ox-4	0.10±0.01	0.096±0.003
Ox-5	0.98±0.03	0.968±0.018
Ox-8	0.20±0.01	0.186±0.008
Ox-9	0.47±0.02	0.465±0.012
Ox-11	2.90±0.04	2.94±0.03
Ox-12	6.50±0.38	6.60±0.08
S-2	1.52±0.03	1.53±0.03
KH-1	0.86±0.02	0.85±0.02
WG-2	1.40±0.07	1.38±0.03

[a] Certificates of Analysis for Gold Reference Materials, Rock Labs, Auckland, New Zealand, 1997, 1998 and 1999.

Limit of Detection by Different Methods

The limit of detection using the FA method depends on the amount of sample taken and the type of microbalance used. Samples of 50 g were used for the FA method. The readability of the balance used was 0.1 µg and a stable reading was obtained only around 0.3 µg. The detection limit was found to be 6 ng/g. In the case of instrumental methods, the limit of detection depends on the signal-to-noise ratio. The FAAS method resulted in a detection limit of 60 ng/g. The GFAAS technique with Zeeman background correction not only reduced the background interferences but also gave much better precision (<2% RSD) for background measurements. The detection limit obtained was 0.1 ng/g for GFAAS. This makes ICP-MS the most sensitive method for the estimation of gold in geological samples with a detection limit of 0.01 ng/g.

Accuracy and Precision

Sample non-homogeneity is one of the most important issues in the analysis of gold in geological samples. Ten-gram sample aliquots are found to give values with a precision better than 10% RSD in most cases, showing that a 10-g amount of sample yields reasonably reliable values with comparable accuracy. The precision obtained for international gold reference materials are in most cases even better than 6% RSD. This is obvious because all standards will be sieved and in some instances, the gold nuggets removed by dissolving them in cyanide solution to ensure that there is no gold nugget effect.

In applied geochemical studies, the main objective is to provide results for a large number of samples collected as part of a geochemical mapping project or a geochemical exploration program, although accuracy and precision

TABLE VI
Gold Concentration (ng/g) in International Gold Reference Materials Field and Samples Using GFAAS After MIBK Extraction and ICP-MS Analysis in Comparison to Certified Values

	Au (ng/g)		
Sample	MIBK GFAAS*	ICP-MS (12)	Certified Values (21)
GAu-8	0.7±0.06	0.55±0.05	0.5±0.1
GAu-9	1.4±0.08	1.46±0.15	1.5±0.1
GAu-10	5.2±0.30	5.1±0.46	5.3+0.2
GAu-11	11.8±0.83	11.7±1.10	11.4±0.4
GAu-12	22.4±1.2	22.3±2.0	21.5±1.0
GAu-13	55.7±1.68	52.5±3.0	50.0±2.0
GAu-14	106±3.00	105.0±5.0	100.0±3.0
GAu-15	310±26	318±32	300±20

* Average of six determinations.

TABLE VII
Gold Concentration (µg/g) in Sulfidic-Banded Iron Formation Samples Using Flame AAS in Comparison to Fire Assay Analysis

	Au (µg/g)	
Sample	FAAS [a]	Fire Assay*
Sample 1	2.21±0.20	3.8
Sample 2	0.42±0.02	0.3
Sample 3	0.52±0.04	0.6
Sample 4	0.97±0.07	1.6
Sample 5	1.39±0.11	1.4
Sample 6	4.00±0.20	3.7
Sample 7	0.78±0.07	0.6
Sample 8	0.49±0.04	0.4
Sample 9	0.05±0.01	0.1

[a] Average of three determinations.
* Using 50-g sample, single values.

TABLE VIII
Gold Concentration (µg/g) in Field Samples Using FAAS in Comparison to ICP-MS in Analysis

	Au (µg/g)	
Sample	FAAS*	ICP-MS (12)
TKG-129	0.01±0.01	0.02±0.01
TKG-261	1.41±0.10	1.48±0.13
TKG-263	1.56±0.08	1.76±0.14
TKG-270	2.80±0.09	2.76±0.19
TKG-277	0.21±0.02	0.19±0.01
TKG-321	0.15±0.01	0.17±0.01
RAMC-10	0.11±0.01	0.10±0.01
UT-23	0.24±0.02	0.27±0.02
AJN-1	6.45±0.38	6.70±0.53
AJN-2	9.03±0.72	8.95±0.27
RAMC-1	0.11±0.01	0.09±0.01

* Average of six determinations.

are also always important. Figure 3 presents an error bar chart for the determination of gold in 70 replicate samples of Ox-5 obtained over a period of one year. It can be seen that more than 90% of the values are within acceptable range, demonstrating accuracy of the results.

CONCLUSION

The FAAS method described for the determination of gold is precise, economical, and comparatively simple, but not sensitive enough for low gold concentrations. Since the FAAS limit of quantification for gold is 0.1 ug/g, this method cannot be used in situations where gold concentration is presumed to be at lower levels. The results presented here reveal that this method works well for samples of sulphidic-banded iron formations, quartz veins, quartz vein-bearing volcanic rocks, shaly sulphidic-banded iron formations, and enriched ores which are known to contain higher amounts of gold. On the other hand, for samples having gold below the 100-ng/g level, GFAAS or ICP-MS can be used.

ACKNOWLEDGMENTS

The authors are grateful to Dr.H.K.Gupta, Director, National Geophysical Research Institute, Hyderabad, for permission to publish this work. The guidance and encouragement obtained from Dr. S.M. Naqvi, Head, Geochemistry Division, is deeply acknowledged.

Received June 23, 2000.

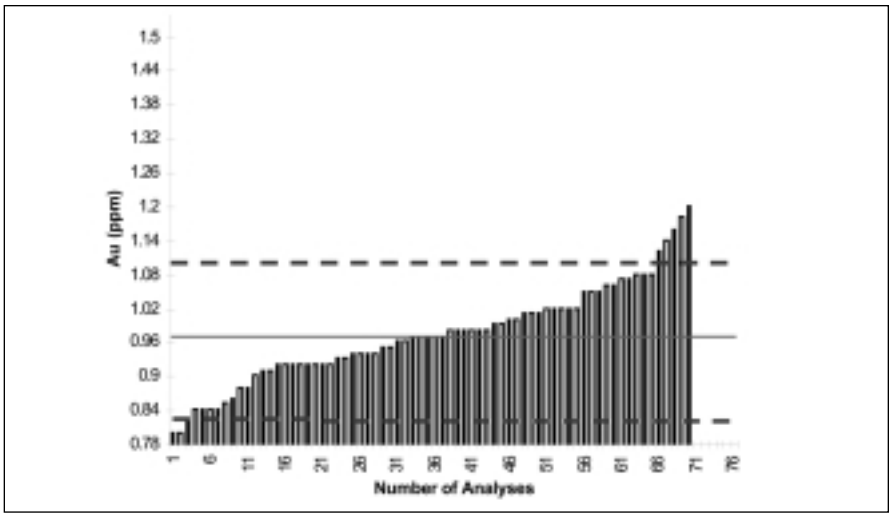

Fig. 3. Error Bar Chart for gold determination of 70 replicate samples of an international gold ore reference material (Ox-5) by FAAS. The concentration of gold in the reference sample is 0.968 + 0.018 µg/g. A precision of about 15% RSD is acceptable at a concentration of 0.968 µg/g gold in applied geochemical studies (Thomson et al. 1996). Hence, the values in the range of 0.968 + 0.145 are acceptable. It can be seen that more than 90% of the values obtained are within the acceptable range.

REFERENCES

1. Manikyamba, C, Naqvi, S.M, Sawkar R.H and Group G.R. Curr. Sci. 72, 515 (1997).
2. Balaram, V. Gnaneswara Rao, T. Anjaiah K.V. and Ramesh S.L. Proc. Nat. Workshop on Exploration and Exploitation of Gold Resources of India, N.G.R.I, Hyderabad, India, 231(1996).
3. Levinson A.A, Introduction to exploration geochemistry, Applied Publishing Ltd, Calgary (1974).
4. Van Loon J.C. and Barefoot R.R., Determination of precious metals - Selected instrumental methods, Wiley, Chichester, pp 276 (1991).
5. Hamilton E.A., Manual of Cyanidation, McGraw-Hill, New York pp 276 (1920).
6. Fletcher K and Horsky S, J. Geochem. Explor. 30, 29 (1998).
7. Greonewald, T, Anal. Chem., 41, 1012 (1969).
8. Rubeska I, Thomas V.A, Baby T.V. and Thomas, O, Interim Report CH-5, Mineral exploration and development in Kerala, UN Assisted Project, Trivandrum, India 1-12 (1980).
9. Tewari R.K, Tarsekar V.K and Lokhande M.B, At. Spectrosc. 11, 125 (1990).
10. Benedetti M.F, Dekersabiec A.M. and Boulegue J, Geostand Newsl.. 11,127 (1987).
11. Yan M, Wang C, CaQ, Gu T and Cli Q,Geostand. Newsl. 19, 2, 125 (1995).
12. Balaram V and Anjaiah K.V., J. Indian Chem Soc. 74, 581 (1997).
13. Barefoot R.R., J. Anal At. Spectrom. 13, 1077 (1998).
14. Elson, O.M. and Chatt A, Anal. Chim. Acta. 155, 305 (1983).
15. Balaram V, Sunder Raju, P.V., Ramesh, S.L. , Anjaiah, K.V., Dasram B, Manikyamba, C. Ram Mohan, M. and Sarma D.S., At. Spectrosc. 20, 4 (1999).
16. Balaram V, Hussain S.M., Uday Raj, Charan S.N, Subba Rao D.V., Anjaiah K.V, Ramesh S.L and Illangovan S, At. Spectrosc. 18, 17 (1997).
17. Clifton H.E., Hunter R.K., Swanson F.T and Phillips, R.L, U.S. Geol. Surv. Pap. 625, C pp 17 (1969).
18. Latinser W.M and Hildebrand J.H, Reference book of inorganic chemistry, The Macmillian Company, New York, p. 206 (1940).
19. Beamish F.E and Van Loon J.C, Analysis of noble metals overview and selected methods" Academic Press, New York (1972).
20. Thompson M., Potts, P.J. and Webb P.C., Geostand. Newsl. 20, 295 (1995).
21. Mingcai Y., Chumshu, W., Qunxian C., Tioxin G and Qinghua C., Geostand. Newsl. 19, 125 (1995).

New Book on Graphite Furnace AA

Analytical Graphite Furnace Atomic Absorption Spectrometry
A Laboratory Guide
by G. Schlemmer and B. Radziuk

This book is a laboratory guide that provides profound and practical insight into the physical and technical background of graphite furnace AA and its perfect use for routine analysis. The reader is guided from sample pretreatment via calibration and validation of the instrument to the use of accessories and software in modern graphite furnace AA.

The authors have been involved in basic and applications research for more than two decades, in addition to teaching user-training courses and providing technical support.

To order a copy of the book, Part No. B051-1731, please contact:

PerkinElmer Bodenseewerk
Postfach 101761
D-88647 Überlingen, Germany
Tel: (+49) (0) 7551 810
Fax: (+49) (0) 7551 2954

For subscription information or back issues, write or fax:

Atomic Spectroscopy
P.O. Box 3674
Barrington, IL 60011 USA
Fax: (+1) 847-304-6865

To submit articles for publication, write or fax:

Editor, Atomic Spectroscopy
PerkinElmer Instruments
761 Main Avenue
Norwalk, CT 06859-0226 USA
Fax: (+1) 203-761-2898